macular degeneration or cone-rod degeneration. *Invest Ophthalmol Vis Sci.* 2001;42:2229-2236.

20. Fumagalli A, Ferrari M, Soriani N, et al. Mutational scanning of the ABCR gene with double-gradient denaturing-gradient gel electrophoresis (DG-DGGE) in Italian Stargardt disease patients. *Hum Genet.* 2001;109:326-338.
21. Shroyer NF, Lewis RA, Yatsenko AN, Wensel TG, Lupski JR. Cosegregation and functional analysis of mutant ABCR (ABCA4) alleles in families that manifest both Stargardt disease and age-related macular degeneration. *Hum Mol Genet.* 2001; 10:2671-2678.
22. Klevering BJ, Blankenagel A, Maugeri A, Cremers FP, Hoyng CB, Rohrschneider K. Phenotypic spectrum of autosomal recessive cone-rod dystrophies caused by mutations in the ABCA4 (ABCR) gene. *Invest Ophthalmol Vis Sci.* 2002;43: 1980-1985.
23. Pang CP, Lam DS. Differential occurrence of mutations causative of eye diseases in the Chinese population. *Hum Mutat.* 2002;19:189-208.
24. Stenirri S, Fermo I, Battistella S, et al. Denaturing HPLC profiling of the ABCA4 gene for reliable detection of allelic variations. *Clin Chem.* 2004;50:1336-1343.
25. Downs K, Zacks DN, Caruso R, et al. Molecular testing for hereditary retinal disease as part of clinical care. *Arch Ophthalmol.* 2007;125:252-258.
26. Ernest PJ, Boon CJ, Klevering BJ, Hoefsloot LH, Hoyng CB. Outcome of ABCA4 microarray screening in routine clinical practice. *Mol Vis.* 2009;15:2841-2847.
27. Xi Q, Li L, Traboulsi EI, Wang QK. Novel ABCA4 compound heterozygous mutations cause severe progressive autosomal recessive cone-rod dystrophy presenting as Stargardt disease. *Mol Vis.* 2009;15:638-645.
28. Littink KW, Koenekoop RK, van den Born LI, et al. Homozygosity mapping in patients with cone-rod dystrophy: novel mutations and clinical characterizations. *Invest Ophthalmol Vis Sci.* 2010;51:5943-5951.
29. Maugeri A, van Driel MA, van de Pol DJ, et al. The 2588G->C mutation in the ABCR gene is a mild frequent founder mutation in the Western European population and allows the classification of ABCR mutations in patients with Stargardt disease. *Am J Hum Genet.* 1999;64:1024-1035.
30. Klevering BJ, Yzer S, Rohrschneider K, et al. Microarray-based mutation analysis of the ABCA4 (ABCR) gene in autosomal recessive cone-rod dystrophy and retinitis pigmentosa. *Eur J Hum Genet.* 2004;12:1024-1032.
31. Fujinami K, Sergouniotis PI, Davidson AE, et al. The clinical effect of homozygous ABCA4 alleles in 18 patients [published online ahead of print June 11, 2013]. *Ophthalmology.* doi:10.1016/j.ophtha.2013.04.016.
32. Sergouniotis PI, Davidson AE, Lenassi E, Devery SR, Moore AT, Webster AR. Retinal structure, function, and molecular pathologic features in gyrate atrophy. *Ophthalmology.* 2012; 119:596-605.
33. Bach M, Brigell MG, Hawlina M, et al. ISCEV standard for clinical pattern electroretinography (PERG): 2012 update. *Doc Ophthalmol.* 2013;126:1-7.
34. Marmor MF, Fulton AB, Holder GE, Miyake Y, Brigell M, Bach M. ISCEV standard for full-field clinical electroretinography (2008 update). *Doc Ophthalmol.* 2009;118:69-77.
35. Lois N, Holder GE, Bunce C, Fitzke FW, Bird AC. Phenotypic subtypes of Stargardt macular dystrophy-fundus flavimaculatus. *Arch Ophthalmol.* 2001;119:359-369.
36. Ng PC, Henikoff S. SIFT: predicting amino acid changes that affect protein function. *Nucleic Acids Res.* 2003;31:3812-3814.
37. Adzhubei IA, Schmidt S, Peshkin L, et al. A method and server for predicting damaging missense mutations. *Nat Methods.* 2010;7:248-249.
38. den Dunnen JT, Antonarakis SE. Mutation nomenclature extensions and suggestions to describe complex mutations: a discussion. *Hum Mut.* 2000;15:7-12.
39. Braun TA, Mullins RF, Wagner AH, et al. Non-exomic and synonymous variants in ABCA4 are an important cause of Stargardt disease. *Hum Mol Genet.* In press.
40. Burke TR, Allikmets R, Smith RT, Gouras P, Tsang SH. Loss of peripapillary sparing in non-group I Stargardt disease. *Exp Eye Res.* 2010;91:592-600.
41. Fritsche LG, Fleckenstein M, Fiebig BS, et al. A subgroup of age-related macular degeneration is associated with monoallelic sequence variants in the ABCA4 gene. *Invest Ophthalmol Vis Sci.* 2012;53:2112-2118.

Investigative Ophthalmology & Visual Science

the fovea in one patient, and a lack of peripapillary sparing on AF imaging in three subjects. In this study, patients with bilateral macular atrophy, with or without surrounding flecks, potentially were included as having Stargardt disease, with other less typical ("atypical") findings also having been reported in *ABCA4*-associated retinal disease.[18,40,41] However, other genes associated with autosomal recessive macular dystrophy, autosomal recessive cone-rod dystrophy, and autosomal recessive retinitis pigmentosa also should be considered for these patients with no identified likely disease-causing *ABCA4* alleles, in addition to the possibility of missed *ABCA4* alleles due to the inherent limitations of the molecular testing approach.

In our cohort, in keeping with previous reports, there was one well-known intronic variant (c.5461-10T>C) of equivocal pathogenicity following detailed in silico analysis,[4,5,16]; highlighting the need for an effective assay to determine functionally the effects of *ABCA4* variants, or alternatively to consider investigating mRNA expression. The allele, c.5461-10T>C, was the most common in our cohort, with 8/79 patients (10%) harboring this variant. Interestingly, the second allele was not identified in six of these patients. However, co-segregation of c.5461-10T>C with the disease has been documented in several studies, thereby strongly suggesting its disease-causation.[4]

In summary, we have demonstrated the validity and utility of *ABCA4* mutation screening with an NGS-based protocol in a large British cohort, with successful identification of the new disease-causing alleles in approximately half of the cases harboring one allele detected by prescreening with APEX technology. The identification of both disease-causing alleles will improve the accuracy of diagnosis and the counselling of patients, and also will assist in more effective patient selection of genetically confirmed participants for current and future clinical trials for *ABCA4*-associated retinal disease.

Acknowledgments

The authors thank the patients who kindly agreed to take part in this study and colleagues who referred individuals to us at Moorfields Eye Hospital, and those who contributed to the assembly of the *ABCA4* panel, particularly Naushin Waseem, Bev Scott, and Sophie Devery. The authors also thank Graham E. Holder, Anthony G. Robson, and Magella M. Neveu for interpretation of electrophysiologic data, and Yozo Miyake, Arundhati Dev Borman, Rajarshi Mukherjee, Eva Lenassi, Panagiotis I. Sergouniotis, and Aman Chandra for their insightful comments.

Supported by grants from the National Institute for Health Research Biomedical Research Centre at Moorfields Eye Hospital NHS Foundation Trust and UCL Institute of Ophthalmology; Foundation Fighting Blindness (USA); Fight For Sight; Moorfields Eye Hospital Special Trustees; Macular Disease Society; National Eye Institute/NIH Grants EY021163, EY019861, and EY019007 (Core Support for Vision Research); unrestricted funds from Research to Prevent Blindness (New York, NY) to the Department of Ophthalmology; Columbia University; Suzuken Memorial Foundation; Mitsukoshi Health and Welfare Foundation; Daiwa Anglo-Japanese Foundation; and Grant-in-Aid for Young Scientists (B) of the Ministry of Education, Culture, Sports, Science, and Technology (Japan); and by a Foundation Fighting Blindness Career Development Award (MM). The authors alone are responsible for the content and writing of the paper.

Disclosure: **K. Fujinami**, None; **J. Zernant**, None; **R.K. Chana**, None; **G.A. Wright**, None; **K. Tsunoda**, None; **Y. Ozawa**, None; **K. Tsubota**, None; **A.R. Webster**, None; **A.T. Moore**, None; **R. Allikmets**, None; **M. Michaelides**, None

References

1. Allikmets R, Singh N, Sun H, et al. A photoreceptor cell-specific ATP-binding transporter gene (ABCR) is mutated in recessive Stargardt macular dystrophy. *Nat Genet.* 1997;15:236–246.
2. Michaelides M, Chen LL, Brantley MA Jr, et al. ABCA4 mutations and discordant ABCA4 alleles in patients and siblings with bull's-eye maculopathy. *Br J Ophthalmol.* 2007;91:1650–1655.
3. Burke TR, Tsang SH. Allelic and phenotypic heterogeneity in ABCA4 mutations. *Ophthalmic Genet.* 2011;32:165–174.
4. Fujinami K, Lois N, Davidson AE, et al. A longitudinal study of Stargardt disease: clinical and electrophysiological assessment, progression and genotype correlations. *Am J Ophthalmol.* 2013;155:1075–1088.
5. Zernant J, Schubert C, Im KM, et al. Analysis of the ABCA4 gene by next-generation sequencing. *Invest Ophthalmol Vis Sci.* 2011;52:8479–8487.
6. Fujinami K, Akahori M, Fukui M, Tsunoda K, Iwata T, Miyake Y. Stargardt disease with preserved central vision: identification of a putative novel mutation in ATP-binding cassette transporter gene. *Acta Ophthalmol.* 2011;89:297–298.
7. Webster AR, Heon E, Lotery AJ, et al. An analysis of allelic variation in the ABCA4 gene. *Invest Ophthalmol Vis Sci.* 2001;42:1179–1189.
8. Cremers FP, van de Pol DJ, van Driel M, et al. Autosomal recessive retinitis pigmentosa and cone-rod dystrophy caused by splice site mutations in the Stargardt's disease gene ABCR. *Hum Mol Genet.* 1998;7:355–362.
9. Martinez-Mir A, Paloma E, Allikmets R, et al. Retinitis pigmentosa caused by a homozygous mutation in the Stargardt disease gene ABCR. *Nat Genet.* 1998;18:11–12.
10. Rozet JM, Gerber S, Souied E, et al. Spectrum of ABCR gene mutations in autosomal recessive macular dystrophies. *Eur J Hum Genet.* 1998;6:291–295.
11. Lewis RA, Shroyer NF, Singh N, et al. Genotype/phenotype analysis of a photoreceptor-specific ATP-binding cassette transporter gene, ABCR, in Stargardt disease. *Am J Hum Genet.* 1999;64:422–434.
12. Rozet JM, Gerber S, Ghazi I, et al. Mutations of the retinal specific ATP binding transporter gene (ABCR) in a single family segregating both autosomal recessive retinitis pigmentosa RP19 and Stargardt disease: evidence of clinical heterogeneity at this locus. *J Med Genet.* 1999;36:447–451.
13. Yatsenko AN, Shroyer NF, Lewis RA, Lupski JR. Late-onset Stargardt disease is associated with missense mutations that map outside known functional regions of ABCR (ABCA4). *Hum Genet.* 2001;108:346–355.
14. Jaakson K, Zernant J, Kulm M, et al. Genotyping microarray (gene chip) for the ABCR (ABCA4) gene. *Hum Mutat.* 2003;22:395–403.
15. Fishman GA, Stone EM, Grover S, Derlacki DJ, Haines HL, Hockey RR. Variation of clinical expression in patients with Stargardt dystrophy and sequence variations in the ABCR gene. *Arch Ophthalmol.* 1999;117:504–510.
16. Papaioannou M, Ocaka L, Bessant D, et al. An analysis of ABCR mutations in British patients with recessive retinal dystrophies. *Invest Ophthalmol Vis Sci.* 2000;41:16–19.
17. Rivera A, White K, Stohr H, et al. A comprehensive survey of sequence variation in the ABCA4 (ABCR) gene in Stargardt disease and age-related macular degeneration. *Am J Hum Genet.* 2000;67:800–813.
18. Birch DG, Peters AY, Locke KL, Spencer R, Megarity CF, Travis GH. Visual function in patients with cone-rod dystrophy (CRD) associated with mutations in the ABCA4(ABCR) gene. *Exp Eye Res.* 2001;73:877–886.
19. Briggs CE, Rucinski D, Rosenfeld PJ, Hirose T, Berson EL, Dryja TP. Mutations in ABCR (ABCA4) in patients with Stargardt

TABLE 6. Distribution of 79 Patients With *ABCA4*-Related Retinal Disease Based on Number of Identified Disease-Causing Variants

		Comprehensive Screening With APEX and NGS			
		No Disease-Causing Variant	1 Disease-Causing Variant	2 Disease-Causing Variants	3 Disease-Causing Variants
Prescreening with APEX	1 disease causing-variant, $n = 66$		29	36	1
	No disease-causing variants, $n = 13$	6	7		
	Total, $n = 79$	6	36	36	1

A total of 42 additional variants, which were not detected by APEX, were identified in 45 (57%) patients screened by NGS (Tables 2, 4). Three variants (p.R219*, p.R1108C, and p.S1071fs) found by NGS, were not identified by APEX at the prescreening stage despite being represented on the array ("APEX false-negative"; Table 2, patients 11, 16, 25, and 61). Three (3/45) subjects had two new variants and 42 (42/45) individuals had one new variant (Table 2). Of the 42 new variants detected by NGS, there were 23 missense, 9 splice-site alterations, 6 nonsense, 3 frameshifts, and 1 in-frame deletion (Table 4).

Of the 42 new variants identified by NGS, 33 (79%) were novel, including 18 missense, 7 splice-site alterations, 4 nonsense, 3 frameshifts, and 1 in-frame deletion (Tables 2, 4, 5). Seven variants identified only by NGS already were known, but not yet added to the *ABCA4* array by the time of the prescreening of those samples.

In Silico Molecular Genetic Analysis for New Variants Identified by NGS

In silico analysis of the 42 variants identified by NGS, including the 9 previously reported variants and the 33 novel variants, are shown in Tables 3 and 5, respectively.

Of the 9 previously reported variants that were detected by NGS, there were 4 null variants (2 nonsense and 2 splice-site alterations); 4 disease-causing missense variants, with deleterious or damaged protein function predicted by SIFT and Polyphen2; and one benign missense variant (p.D2177N, Table 3).

Deleterious or damaged protein function was predicted by SIFT and Polyphen2 in 16 of 18 novel missense variants (Table 5). Two variants (p.I478T and p.K896E) were predicted to be tolerated and benign. The predicted effects on splicing of these 16 missense variants, one variant resulting in a nucleotide substitution at the end of exon 33 (c.4773G>C), and five intronic variants, were assessed using the HSF program. Altered splicing was suggested for 7 of the missense variants, the (c.4773G>C) variant, and all 5 intronic variants (Table 5). The allele frequencies for the 33 novel variants were, at most, 1 in 13006, suggesting that these are all very rare. Overall, 31 of the 33 novel variants were considered disease-causing, except for only the two missense variants, p.I478T and p.K896E (Table 5).

Disease-Causing Variants

A total of 73 (31 novel and 42 previously identified) disease-causing variants was identified in this cohort of 79 patients (Table 4). The distribution of the number of alleles in the cohort is summarized in Table 6. One patient (1%) harbored three disease-causing variants, 36 (46%) had two disease-causing variants, 36 (46%) had one disease-causing variant, and six patients (7%) remained with no disease-causing variant identified (Table 6).

DISCUSSION

Our study reports the molecular genetic findings using a PCR-enrichment-based NGS strategy in a large well-characterized British cohort with a clinical diagnosis of *ABCA4*-associated retinal disease. The NGS revealed two or more disease-causing variants in 37 (47%) of 79 patients, in whom only one variant was detected in prescreening with APEX array technology.

Of the 66 subjects with one disease-causing allele identified previously by APEX, the second disease-causing allele was identified in 37 individuals (56%). In keeping with our findings, Zernant et al. reported that the same NGS strategy identified the second disease-causing allele in 48% of their cohort who also only had one allele found previously with APEX.[5] These findings suggest that many disease-associated mutations in the *ABCA4* gene are very rare and yet unknown, supporting the validity of the PCR-enrichment-based NGS method either as the screening method of choice, or as an additional screening method for patients in whom APEX does not reveal two variants. Of note, the NGS method is cost- and time-efficient at this time only for large (at least 96 samples) cohorts.

Of the 13 patients with initially no disease-causing variant found by APEX, one disease-causing *ABCA4* allele was identified in seven subjects (54%) by NGS, with six remaining with no likely disease-causing allele (46%). Further screening with NGS, including screening all intronic regions, and upstream and downstream control regions of the *ABCA4* gene, as well as other candidate genes, in larger well-characterized cohorts will be needed to identify fully all pathogenic alleles in these patients. It recently has been proposed that intronic and synonymous variants may account for a significant proportion of the remaining disease-causing variants not identified with exomic NGS.[5,39]

There were two "NGS false negative" variants (p.R1129H and p.Q1513fs) and three "APEX false negative" variants (p.R219*, p.R1108C, and p.S1071fs) in our cohort. The missense variant p.R1129H was not detected by NGS, most likely due to allele-specific amplification. The frameshift variant c.4537_4538insC, p.Q1513fs, is located in a homopolymer of seven C-nucleotides, where an insertion of another C nucleotide presents a challenge to identify by the Roche 454 sequencing platform. The "APEX false negative" variants were caused by technical issues with the specific array, ABCR400 (432 mutations on the chip) in 2005. Two of those variants, p.R1108C, and p.S1071fs, were detected by APEX in other patients (Table 2). Nevertheless, these findings suggest that combined APEX/NGS analysis may be worthy of consideration for comprehensive mutation detection.

In silico molecular genetic analysis was performed for all 84 variants identified in our cohort, with 73 of these determined to be likely disease-causing. Review of the clinical findings of the six patients harboring only one, likely benign, missense variant, revealed that they had a less typical ("atypical") phenotype for *ABCA4*-associated retinal disease, including an absence of flecks in all patients, significant peripheral retinal bone spicule pigmentation in three subjects, geographic-like atrophy in one individual, a subtle atrophic change confined to

TABLE 5. Continued

Exon/ IVS	DNA Change	Protein Change/ Effect	N of Alleles Identified	Pt	SIFT Pred.	SIFT Tol. Index (0–1)	Polyphen2 Pred.	Polyphen2 Hum Var Score (0–1)	HSF Matrix Site	HSF Matrix Wt CV	HSF Matrix Mt CV	HSF Matrix CV % Variation	Allele Freq. by EVS	Reference	Comments
33	c.4773G>C	Splice site	1	29					Don.	84.58	73.57	Site broken (−13.02)	ND		
35	c.4978delC	p.L1661*	1	24									ND		
36	c.5041_5055del GTGGTTGCCATCTGC	p.V1681_C1685del	1	40								NA	ND	db SNP (rs62646872)	
36	c.5088C>G	p.S1696R	1	10	Tol.	NA	PRD	0.780	Don.	59.34	86.17	New site (45.23)	ND		
39	c.5578C>T	p.R1860W	1	38	Del.	0.02	B	0.025				No change	ND	db SNP (rs200849015)	
IVS42	c.5899-3_ 5899-2delTA	Splice site	1	66								NA	ND		
IVS42	c.5899-2delA	Splice site	1	58					Acc.	82.1	28.26	WT site broken (−65.58)	ND		
45	c.6209C>G	p.T2070R	1	52	Tol.	NA	PRD	0.996	Acc.	57.41	86.36	New site (50.42)	ND		
46	c.6385A>G	p.S2129G	1	43	Del.	NA	B	0.001					ND		Possibly disease-causing

Splice-site alteration (described as splice site) includes the change expected to affect splicing, for example, when the splice donor or splice acceptor site is changed, and the change that might affect splicing, for example, changes close to the splice donor or splice acceptor site, or in the first or last nucleotide of an exon. SIFT (version 4.0.4) results are reported to be tolerant if tolerance index is ≥0.05 or deleterious if tolerance index is <0.05. Polyphen-2 (vision 2.1) appraises mutations qualitatively as benign, possibly damaging or probably damaging based on the model's false positive rate. The cDNA is numbered according to Ensemble transcript ID ENST00000370225, in which +1 is the A of the translation start codon. Human splicing finder version 2.4.1 was applied to predict the effect of each variant on splicing. The result from the HSF matrix indicates the values for the Wt and mutant sequences. The larger the difference in values between the Wt and the mutant sequences suggests a greater chance that the variant can affect splicing. EVS denotes variants in the Exome Variant Server, NHLBI Exome Sequencing Project, Seattle, WA (accessed 01/04/2013; available in the public domain at http://snp.gs.washington.edu/EVS).

Table 5. In Silico Molecular Genetic Analysis for Novel ABCA4 Variants Identified by NGS

					SIFT		Polyphen2		HSF Matrix						
Exon/ IVS	DNA Change	Protein Change/ Effect	*N* of Alleles Identified	Pt	Pred.	Tol. Index (0–1)	Pred.	Hum Var Score (0–1)	Site	Wt CV	Mt CV	CV % Variation	Allele Freq. by EVS	Reference	Comments
3	c.180delG	p.M61fs	1	35									ND		
IVS7	c.859-9T>C	Splice site	1	5					Acc.	78.18	76.99	Possibly site broken (−1.52)	ND		Possibly disease-causing
11	c.1433T>C	p.I478T	1	1	Tol.		B	0.007				No change	ND		Benign
11	c.1519G>T	p.D507Y	1	20	Del.	0.01	POD	0.641				No change	1/13006	dbSNP (rs148234178)	
12	c.1749G>C	p.K583N	1	68	Del.	0.04	POD	0.893	Acc.	66.17	37.22	Site broken (−43.75)	1/13006	dbSNP (rs145265791)	
14	c.1982_ 1983insG	p.A662fs	1	69									ND		
15	c.2297G>T	p.G766V	1	1	Tol.	NA	POD	0.557	Don.	69.18	42.34	Site broken (−38.79)	ND		
15	c.2345G>A	p.W782*	1	3									ND		
16	c.2510T>C	p.L837P	1	72	Tol.	NA	POD	0.905				No change	ND		
16	c.2568C>A	p.Y856*	1	5									ND		
18	c.2686A>G	p.K896E	1	53	Tol.	NA	B	0.002					ND		Benign
20	c.2942C>T	p.P981L	1	19	Del.	0.00	POD	0.813				No change	1/13006	dbSNP (rs147826775)	
20	c.2972G>T	p.G991V	1	70	Del.	NA	PRD	0.998	Donor	64.62	91.45	New site (41.53)	ND		
IVS20	c.3050+1G>C	Splice site	1	54					Acc.	86.43	57.49	Site broken (−33.49)	ND		
IVS21	c.3191-1G>T	Splice site	1	26					Acc.	94.38	65.44	WT site broken (−30.67)	ND		
22	c.3289A>T	p.R1097*	1	71									ND		
22	c.3299T>A	p.I1100N	1	23	Del.	NA	PRD	0.986				No change	ND		
23	c.3370G>T	p.D1124Y	1	62	Del.	NA	PRD	0.998				No change	ND		
23	c.3392delC/ 3393C>G	p.A1131Gfs	1	55									ND		
23	c.3398T>C	p.I1133T	1	27	Del.	NA	B	0.100				No change	ND		Possibly disease-causing
27	c.4070C>A	p.A1357E	1	28	Del.	NA	PRD	0.94	Acc.	40.92	69.86	New site (+70.74)	ND		
IVS30	c.4539+2T>G	Splice site	1	56					Don.	79.18	52.35	WT site broken (−33.89)	ND		
31	c.4552A>C	p.S1518R	1	57	Del.	NA	POD	0.871	Acc.	76.3	47.36	Site broken (−37.94)	ND		
31	c.4634G>A	p.S1545N	2	21, 25	Tol.	NA	B	0.253	Acc.	80.04	51.1	Site broken (−36.16)	ND		

TABLE 4. Numbers and Types of Variants Detected by APEX Technology and NGS

		Null				Non-Null		
	Total	Splice-Site Altering	Nonsense	Frameshift	Unknown	In-Frame Deletion	Disease-Causing Missense	Benign Missense
Variants detected by prescreening with APEX	42	4	4	2	1	0	23	8
New variants detected by NGS alone	42 (33)	9 (7)	6 (4)	3 (3)	0 (0)	1 (1)	20 (16)	3 (2)
Gross total	84 (33)	13 (7)	10 (4)	5 (3)	1 (0)	1 (1)	43 (16)	11 (2)

Numbers in parentheses indicate the numbers of novel variants that have never been reported. Two variants were detected only on APEX array, but not identified by NGS; one frameshift variant (p.Q1513fs) and one disease-causing missense variant (p.R1129H).

tional generalized cone and rod ERG abnormality (assessed using dark adapted 0.01 dim flash ERG and dark adapted 11.0 bright flash ERG).

Genetic Screening

Blood samples were collected in EDTA tubes and DNA was extracted with a Nucleon Genomic DNA extraction kit (BACC2; Tepnel Life Sciences, Manchester, UK). Mutation prescreening of *ABCA4* was performed with the APEX microarray (ABCR400 chip or ABCR600 chip; Asper Ophthalmics, Tartu, Estonia; available in the public domain at http://www.asperbio.com/genetic-tests/panel-of-genetic-tests/stargardt-disease-cone-rod-dystrophy-abca4) in all probands.[14] We screened 17 patients with ABCR400 (432 mutations on the chip) in 2005, 32 with updated ABCR400 (456 mutations) in 2006, 3 with further updated ABCR400 (480 mutations) in 2007, and 27 with ABCR500 (552 mutations) in 2011.

All 50 *ABCA4* exons and exon-intron boundaries were amplified with tagged PCR primers using an amplicon tagging protocol (Access Array; Fluidigm, South San Francisco, CA; available in the public domain at http://www.fluidigm.com/products/access-array.html) and NGS on the Roche 454 platform (Roche Applied Science, Penzberg, Upper Bavaria, Germany) was performed as reported previously.[5] Sequences of the barcoded samples were analyzed with the NextGENE software for next generation sequence analysis (SoftGenetics, State College, PA), which mapped reads to the reference genome (HG19) and identified all the differences compared to the reference sequence. All the identified variants were confirmed by Sanger sequencing. Segregation analysis was not performed in this study.

In Silico Molecular Genetic Analysis

All the missense variants identified were analyzed using two software prediction programs: Sorting Intolerant From Tolerant (SIFT; available in the public domain at http://sift.jcvi.org),[36] and PolyPhen2 (available in the public domain at http://genetics.bwh.harvard.edu/pph/index.html).[37] Predicted effects on splicing of all the missense and intronic variants were assessed with the Human Splicing Finder (HSF) program version 2.4.1 (available in the public domain at http://www.umd.be/HSF). The allele frequency of all the variants was estimated by reference to the Exome Variant Server (EVS; NHLBI Exome Sequencing Project, Seattle, WA; available in the public domain at http://snp.gs.washington.edu/EVS).

All the variants identified were classified into one of three categories based on the bioinformatics prediction protocol described in a previous report,[5] namely disease-causing, possibly disease-causing, and benign. For the purpose of analysis in this study, variants predicted to be possibly disease-causing were included in the total number of variants described as disease-causing variants. The nomenclature of the variants was in the main in keeping with the internationally established guidelines (available in the public domain at http://www.hgvs.org/mutnomen).[38]

RESULTS

Clinical Findings

The clinical findings of the cohort are summarized in Table 1. The study included 40 male (51%) and 39 female (49%) unrelated probands. The median age at onset was 22.0 years, with a median duration of disease of 10.0 years. The median age at the latest examination was 40.0 years, with the median logMAR visual acuities being 1.00. Color fundus photographs were obtained in 75 patients and AF imaging was undertaken in 71 subjects. There were 21 patients (30%) with a type 1 AF pattern, 34 (48%) with type 2, and 16 (22%) with type 3. Of the 70 patients with available electrophysiologic data, 34 subjects (49%) were in ERG group 1 (isolated macular dysfunction), 7 (10%) in ERG group 2 (macular and generalized cone dysfunction), and 29 (41%) in ERG group 3 (macular and generalized cone and rod dysfunction).

Color fundus photographs, AF images, and SD-OCT of three representative cases of "typical" *ABCA4*-associated retinal disease are shown in Figure 1 (patients 19, 36, and 17), all harboring two disease-causing variants. Six cases with an "atypical" phenotype for *ABCA4*-associated retinal disease are shown in Figure 2 (patients 74–79), all of them carried only one, likely benign, *ABCA4* variant (Table 2).

Prescreening With APEX Technology

The results of prescreening of *ABCA4* in our cohort of 79 patients are summarized in Table 2. We detected 42 variants at the APEX prescreening stage. In silico analysis of these 42 variants suggested that 34 were disease-causing and 8 were considered benign. Therefore, these analyses confirmed at least one disease-causing variant in 66/79 patients, while 13/79 subjects had no disease-causing variants (Tables 2, 3).

Identification of New Variants by NGS

The results of NGS screening in our cohort of 79 patients are summarized in Table 2. We identified 82 variants by NGS in total; 53 missense, 13 splice-site alterations, 10 nonsense, four frameshifts, one in-frame deletion, and one intronic variant of unknown effect (Tables 2, 4). Of a total of 84 different variants identified in this study by APEX and NGS, there were two "NGS false-negative" variants (p.R1129H and p.Q1513fs), which were detected on APEX array, but were not detected by NGS (Table 2, patients 25 and 38).

TABLE 3. Continued

Exon/ IVS	Nucleotide Substitution	Protein Change/ Effect	*N* of Alleles Identified	Pt	Method		Previous Report	SIFT		Polyphen 2		HSF Matrix				Allele Freq. by EVS	Reference	Comment
					APEX	NGS		Pred.	Tol. Index (0–1)	Pred.	Hum Var Score (0–1)	Wt Site	Wt CV	Mt CV	CV % Variation			
30	c.4537_4538insC	p.G1513fs	1	38	✓		Briggs CE, et al.[19]									ND		False-negative in NGS in patient 38
31	c.4577C>T	p.T1526M	1	39	✓	✓	Lewis RA, et al.[11]	Del.	0.00	PRD	0.910				No change	ND	db SNP (rs61750152)	
33	c.4685T>C	p.I1562T	1	71	✓	✓	Yatsenko, et al.[13]	Tol.	NA	PRD	0.783				No change	ND		Benign
33	c.4715C>T	p.T1572M	1	79	✓	✓	Pang CP and Lamm DS[24]	Del.	0.02	B	0.326				No change	ND	db SNP (rs185093512)	Benign
35	c.4926C>G	p.S1642R	1	40	✓	✓	Birch DG, et al.[22]	Tol.	0.68	B	0.116				No change	ND	db SNP (rs61753017)	
35	c.4956T>G	p.Y1652*	1	41	✓	✓	Fumagalli A, et al.[16]									ND	db SNP (rs61750561)	
IVS35	c.5018+2T>C	Splice site	1	42	✓	✓	APEX					Don.	81.2	54.3	WT site broken (−33.07)	ND		
36	c.5113C>T	p.R1705W	1	7		✓	Ernest PJ, et al.[20]	Del.	NA	PRD	0.996	Don.	46.5	73.3	No change	ND		
IVS38	c.5461-10T>C		8	43, 44, 45, 46, 47, 48, 49, 50	✓	✓	Briggs CE, et al.[19]								No change	3/13006	db SNP (rs1800728)	
IVS39	c.5585-1G>A	Splice site	1	51	✓	✓	Shroyer NF, et al.[21]					Acc.	86.3	57.4	WT site broken (−33.53)	ND		
IVS40	c.5714+5G>A	Splice site	1	52	✓	✓	Cremers FP, et al.[8]					Don.	85.5	73.3	Wild type site broken (−14.23)	ND		
42	c.5882G>A	p.G1961E	7	53, 54, 55, 56, 57, 58, 59	✓	✓	Lewis RA, et al.[11]	Del.	0.00	PRD	0.998				No change	41/13006	db SNP (rs1800553)	
44	c.6079C>T	p.L2027F	4	60, 61, 62, 63	✓	✓	Lewis RA, et al.[11]	Del.	0.00	PRD	1.000				No change	4/13006	db SNP (rs61751408)	
44	c.6089G>A	p.R2030Q	1	64	✓	✓	Lewis RA, et al.[11]	Del.	0.00	PRD	0.995				No change	8/13006	db SNP (rs61750641)	
46	c.6320G>A	p.R2107H	2	72, 73	✓	✓	Fishman GA, et al.[15]	Del.	0.01	PRD	0.999				No change	91/13006	db SNP (rs62642564)	Benign
47	c.6445C>T	p.R2149*	1	65	✓	✓	Lewis RA, et al.[19]									1/13006	db SNP (rs61750654)	
48	c.6529G>A	p.D2177N	1	19		✓	Rivera A, et al.[17]	Tol.	0.41	B	0.004				No change	116/13006	db SNP (rs1800555)	Benign
48	c.6709A>C	p.T2237P	1	66	✓	✓	APEX	Del.	NA	POD	0.719				No change	ND		
IVS48	c.6729+4_+18del AGTTGGCCCTGGGGC	Splice site	1	17		✓	Littink KW, et al.[28]								NA	ND		

Splice-site alteration (described as splice site) includes the change expected to affect splicing, for example, when the splice donor or splice acceptor site is changed, and the change that might affect splicing, for example, changes close to the splice donor or splice acceptor site, or in the first or last nucleotide of an exon. SIFT (version 4.0.4) results are reported to be tolerant if tolerance index is $\geq$0.05 or deleterious if tolerance index is <0.05. Polyphen-2 (vision 2.1) appraises mutations qualitatively as benign, possibly damaging or probably damaging based on the model's false positive rate. The cDNA is numbered according to Ensemble transcript ID ENST00000370225, in which +1 is the A of the translation start codon. Human splicing finder version 2.4.1 was applied to predict the effect of each variant on splicing. The result from the HSF matrix indicates the values for the wild type (Wt) and mutant sequences. The larger the difference in values between the Wt and the mutant sequences suggests a greater chance that the variant can affect splicing. EVS denotes variants in the Exome Variant Server, NHLBI Exome Sequencing Project, Seattle, WA (accessed 01/04/2013; available in the public domain at http://snp.gs.washington.edu/EVS). Acc., Acceptor; Allele freq., allele frequency; CV, consensus values; Del., deleterious; Don., donor; EVS, exome variant server; HSF, human splicing finder; IVS, intervening sequence; Mt, mutant; NA, not available; ND, not detected; POD, possibly damaging; PRD, probably damaging; Pred., prediction; Tol., tolerant.

Table 3. In Silico Analysis for Previously Reported Variants Identified in 79 Patients With ABCA4-Related Retinal Disease

					Method			SIFT		Polyphen 2		HSF Matrix							
Exon/ IVS	Nucleotide Substitution	Protein Change/ Effect	*N* of Alleles Identified	Pt	APEX	NGS	Previous Report	Pred.	Tol. Index (0–1)	Pred.	Hum Var Score (0–1)	Site	Wt CV	Mt CV	CV % Variation	Allele Freq. by EVS	Reference	Comment
3	c.161G>A	p.C54Y	1	1	✓	✓	Lewis RA, et al.[11]	Tol.	0.11	PRD	0.994				No change	1/13006	db SNP (rs150774447)	
3	c.223T>G	p.C75G	1	2	✓	✓	Lewis RA, et al.[11]	Del.	NA	POD	0.605				No change	ND		
5	c.466A>G	p.I156V	2	77, 78	✓	✓	Papaioannou M, et al.[16]	Tol.	0.46	B	0.003				No change	16/13006	db SNP (rs112467008)	Benign
6	c.655A>T	p.R219*	1	11		✓	Xi Q, et al.[27]									ND		
6	c.740A>C	p.N247T	1	3	✓	✓	APEX	Del.	NA	B	0.135				No change	ND		
6	c.768G>T	Splice site	1	4	✓	✓	Klevering BJ, et al.[22]	Tol.	0.56	NA		Don.	70.4	58	Site broken (−17.51)	ND		
9	c.1222C>T	p.R408*	1	5	✓	✓	Webster AR, et al.[7]									ND		
12	c.1726G>C	p.D576H	1	36		✓	Downs K, et al.[45]			POD	0.688	Acc.	68.1	39.1	Site broken (−42.54)	1/13006		
13	c.1804C>T	p.R602W	1	6	✓	✓	Lewis RA, et al.[11]	Del.	0.00	B	0.129				No change	ND	db SNP (rs 6179409)	
13	c.1805G>A	p.R602Q	1	7	✓	✓	Webster AR, et al.[7]	Del.	0.04	PRD	0.513	Acc.	48.9	77.9	New site (+59.14)	2/13006	db SNP (rs61749410)	
13	c.1906C>T	p.Q636*	3	12, 13, 60		✓	Zernant J, et al.[5]								No change	1/13006	db SNP (rs145961131)	
13	c.1922G>C	p.C641S	1	8	✓	✓	Stenirri S, et al.[24]	Del.	0.00						No change	ND	db SNP (rs61749416)	
14	c.1957C>T	p.R653C	2	9, 10	✓	✓	Rivera A, et al.[17]	Del.	0.00	PRD	0.999				No change	ND	db SNP (rs61749420)	
17	c.2588G>C	p.G863A/ p.DelG863	5	11, 12, 13, 14, 15	✓	✓	Lewis RA, et al.[11]/ Maugeri A, et al.[20]	Del.	0.00	PRD	0.996				No change	68/13006	db SNP (rs76157638)	
18	c.2701A>G	p.T901A	1	74	✓	✓	APEX	Tol.	0.82	B	0.008					23/13006	db SNP (rs139655975)	Benign
19	c.2894A>G	p.N965S	1	16	✓	✓	Lewis RA, et al.[11]	Del.	0.03	PRD	0.981	Acc.	53.4	82.3	New site (+54.26)	ND	db SNP (rs201471607)	
20	c.2971G>C	p.G991R	1	67	✓	✓	Yatsenko AN, et al.[13]	Del.	0.02	PRD	0.999				No change	28/13006	db SNP (rs147484266)	Benign
22	c.3064G>A	p.E1022K	2	17, 18	✓	✓	Webster AR, et al.[7]	Del.	0.00	PRD	1.000				No change	ND	db SNP (rs61749459)	
22	c.3208_3209insGT	p.S1071fs	5	19, 20, 21, 22, 25	✓	✓	APEX									ND		False-negative in APEX in patient 25
22	c.3292C>T	p.R1098C	1	23	✓	✓	Rivera A, et al.[17]	Del.	NA	PRD	0.999				No change	ND		
22	c.3322C>T	p.R1108C	3	16, 24, 61	✓	✓	Rozet JM, et al.[10]	Del.	0.00	PRD	0.986				No change	1/13006	db SNP (rs61750120)	False-negative in APEX in patients 16 and 61
23	c.3386G>A	p.R1129H	1	25	✓		Zernant J, et al.[5]			PRD	0.989				No change	ND		False-negative in NGS in patient 25
24	c.3602T>G	p.L1201R	4	72, 73, 74, 79	✓	✓	Lewis RA, et al.[11]	Tol.	0.37	B	0.052	Don.	61.3	73.7	New site (20.08)	416/13006	db SNP (rs61750126)	Benign
28	c.4139C>T	p.P1380L	7	30, 31, 32, 33, 34, 35, 36	✓	✓	Lewis RA, et al.[11]	Del.	0.01	B	0.377				No change	2/13006	db SNP (rs61750130)	
28	c.4234C>T	p.Q1412*	1	33	✓	✓	Rivera A, et al.[17]									ND	db SNP (rs61750137)	
29	c.4283C>T	p.T1428M	1	76	✓	✓	APEX	Tol.	0.15	B	0.010				No change	2/13006	db SNP (rs1800549)	Benign
29	c.4319T>C	p.F1440S	1	34	✓	✓	Lewis RA, et al.[11]	Del.	0.00	POD	0.744				No change	ND	dbSNP (rs61750141)	
29	c.4326C>A	p.N1442K	1	64		✓	Zernant J, et al.[5]	Tol.	NA	POD	0.374				No change	ND		
29	c.4328G>A	p.R1443H	1	35	✓	✓	Rivera A, et al.[17]	Del.	0.02	PRD	0.999				No change	1/13006	dbSNP (rs61750142)	
IVS29	c.4352+1G>A	Splice site	1	73		✓	Zernant J, et al.[5]					Don.	82.3	55.4	WT site broken (−32.62)	ND		
30	c.4469G>A	p.C1490Y	2	36, 37	✓	✓	Lewis RA, et al.[11]	Del.	0.00	PRD	0.994				No change	ND	dbSNP (rs61751402)	
30	c.4538A>G	p.Q1513R	1	67		✓	Webster AR, et al.[7]	Tol.	NA	Benign	0.043	Acc.	91.7	62.8	Site broken (−31.55)	ND		

TABLE 2. Continued

Pt	Allele 1 Detected by APEX			Allele 2 Detected by NGS			Allele 3 Detected by NGS			Total *N* of DC Variants	Comments
	DNA Change	Protein Change/ Effect	Pred. Patho.	DNA Change	Protein Change/ Effect	Pred. Patho.	DNA Change	Protein Change/ Effect	Pred. Patho.		
40	c.4926C>G	p.S1642R	DC	*c.5041_5055del* GTGGTTGCCATCTGC	*p.V1681_C1685del*	DC				2	
41	c.4956T>G	p.Y1652*	DC							1	
42	c.5018+2T>C	Splice site	DC							1	
43	c.5461-10T>C		DC	*c.6385A>G*	*p.S2129G*	PDC				2	
44	c.5461-10T>C		DC							1	
45	c.5461-10T>C		DC							1	
46	c.5461-10T>C		DC							1	
47	c.5461-10T>C		DC							1	
48	c.5461-10T>C		DC							1	
49	c.5461-10T>C		DC							1	
50	c.5461-10T>C		DC							1	
51	c.5585-1G>A	Splice site	DC							1	
52	c.5714+5G>A	Splice site	DC	*c.6209C>G*	*p.T2070R*	DC				2	
53	c.5882G>A	p.G1961E	DC	*c.2686A>G*	*p.K896E*	B				1	
54	c.5882G>A	p.G1961E	DC	*c.3050+1G>C*	*Splice site*	DC				2	
55	c.5882G>A	p.G1961E	DC	*c.3392delC/3393C>G*	*p.A1131Gfs*	DC				2	
56	c.5882G>A	p.G1961E	DC	*c.4539+2T>G*	*Splice site*	DC				2	
57	c.5882G>A	p.G1961E	DC	*c.4552A>C*	*p.S1518R*	DC				2	
58	c.5882G>A	p.G1961E	DC	*c.5899-2delA*	*Splice site*	DC				2	
59	c.5882G>A	p.G1961E	DC							1	
60	c.6079C>T	p.L2027F	DC	c.1906C>T	p.Q636*	DC				2	
61	c.6079C>T	p.L2027F	DC	c.3322C>T	p.R1108C	DC				2	Allele 2 (p.R1108C) was APEX-false-negative
62	c.6079C>T	p.L2027F	DC	*c.3370G>T*	*p.D1124Y*	DC				2	
63	c.6079C>T	p.L2027F	DC							1	
64	c.6089G>A	p.R2030Q	DC	c.4326C>A	p.N1442K	DC				2	
65	c.6445C>T	p.R2149*	DC							1	
66	c.6709A>C	p.T2237P	DC	*c.5899-3_5899-2delTA*	*Splice site*	DC				2	
67	c.2971G>C	p.G991R	B	c.4538A>G	p.Q1513R	DC				1	
68	c.3602T>G	p.L1201R	B	*c.1749G>C*	*p.K583N*	DC				1	
69	c.3602T>G	p.L1201R	B	*c.1982_1983insG*	*p.A662fs*	DC				1	
70	c.3602T>G	p.L1201R	B	*c.2972G>T*	*p.G991V*	DC				1	
71	c.4685T>C	p.I1562T	B	*c.3289A>T*	*p.R1097**	DC				1	
72	c.6320G>A	p.R2107H	B	*c.2510T>C*	*p.L837P*	DC				1	
73	c.6320G>A	p.R2107H	B	c.4352+1G>A	Splice site	DC				1	
74	c.2701A>G	p.T901A	B							0	
75	c.3602T>G	p.L1201R	B							0	
76	c.4283C>T	p.T1428M	B							0	
77	c.466A>G	p.I156V	B							0	
78	c.466A>G	p.I156V	B							0	
79	c.4715C>T	p.T1572M	B							0	

Putative novel variants are shown in italics. Splice-site alteration (described as splice site) includes the change expected to affect splicing, for example, when the splice donor or splice acceptor site is changed, and the change that might affect splicing, for example, changes close to the splice donor or splice acceptor site, or in the first or last nucleotide of an exon. Two variants result in nucleotide substitution at the end of an exon and cause splice-site alteration (c.768G>T and c.4773G>C). B, benign; DC, disease-causing; PDC, possibly disease-causing; Pred. Patho, predicted pathogenicity; Pt, patient number.

TABLE 2. Molecular Genetic Status Identified by NGS in 79 Patients With *ABCA4*-Related Retinal Disease

	Allele 1 Detected by APEX			Allele 2 Detected by NGS			Allele 3 Detected by NGS				
Pt	DNA Change	Protein Change/ Effect	Pred. Patho.	DNA Change	Protein Change/ Effect	Pred. Patho.	DNA Change	Protein Change/ Effect	Pred. Patho.	Total *N* of DC Variants	Comments
1	c.161G>A	p.C54Y	DC	*c.2297G>T*	*p.G766V*	DC				2	
2	c.223T>G	p.C75G	DC	*c.5088C>G*	*p.S1696R*	DC				2	
3	c.740A>C	p.N247T	DC	*c.1433T>C*	*p.I478T*	B	*c.2345G>A*	*p.W782**	DC	2	
4	c.768G>T	Splice site	DC							1	
5	c.1222C>T	p.R408*	DC	*c.2568C>A*	*p.Y856**	DC				2	
6	c.1804C>T	p.R602W	DC	*c.859-9T>C*	*Splice site*	PDC				2	
7	c.1805G>A	p.R602Q	DC	c.5113C>T	p.R1705W	DC				2	
8	c.1922G>C	p.C641S	DC							1	
9	c.1957C>T	p.R653C	DC							1	
10	c.1957C>T	p.R653C	DC							1	
11	c.2588G>C	p.G863A	DC	c.655A>T	p.R219*	DC				2	Allele 2 (p.R219*) was APEX-false-negative
12	c.2588G>C	p.G863A	DC	c.1906C>T	p.Q636*	DC				2	
13	c.2588G>C	p.G863A	DC	c.1906C>T	p.Q636*	DC				2	
14	c.2588G>C	p.G863A	DC							1	
15	c.2588G>C	p.G863A	DC							1	
16	c.2894A>G	p.N965S	DC	c.3322C>T	p.R1108C	DC				2	Allele 2 (p.R1108C) was APEX-false-negative
17	c.3064G>A	p.E1022K	DC	c.6729+4_+18delAGTTGGCCCTGGGGC	Splice site	DC				2	
18	c.3064G>A	p.E1022K	DC							1	
19	c.3208_3209insGT	p.S1071fs	DC	*c.2942C>T*	*p.P981L*	DC	c.6529G>A	p.D2177N	B	2	
20	c.3208_3209insGT	p.S1071fs	DC	*c.1519G>T*	*p.D507Y*	DC				2	
21	c.3208_3209insGT	p.S1071fs	DC	*c.4634G>A*	*p.S1545N*	DC				2	
22	c.3208_3209insGT	p.S1071fs	DC							1	
23	c.3292C>T	p.R1098C	DC	*c.3299T>A*	*p.I1100N*	DC				2	
24	c.3322C>T	p.R1108C	DC	*c.4978delC*	*p.L1661**	DC				2	
25	c.3386G>A	p.R1129H	DC	c.3208_3209insGT	p.S1071fs	DC	*c.4634G>A*	*p.S1545N*	DC	3	Allele 2 (p.S1071fs) was APEX false-negative and allele 1 (p.R1129H) was NGS false-negative
26	c.4139C>T	p.P1380L	DC	*c.3191-1G>T*	*Splice site*	DC				2	
27	c.4139C>T	p.P1380L	DC	*c.3398T>C*	*p.I1133T*	PDC				2	
28	c.4139C>T	p.P1380L	DC	*c.4070C>A*	*p.A1357E*	DC				2	
29	c.4139C>T	p.P1380L	DC	*c.4773G>C*	*Splice site*	DC				2	
30	c.4139C>T	p.P1380L	DC							1	
31	c.4139C>T	p.P1380L	DC							1	
32	c.4139C>T	p.P1380L	DC							1	
33	c.4234C>T	p.Q1412*	DC							1	
34	c.4319T>C	p.F1440S	DC							1	
35	c.4328G>A	p.R1443H	DC	*c.180delG*	*p.M61fs*	DC				2	
36	c.4469G>A	p.C1490Y	DC	c.1726G>C	p.D576H	DC				2	
37	c.4469G>A	p.C1490Y	DC							1	
38	c.4537_4538insC	p.Q1513fs	DC	*c.5578C>T*	*p.R1860W*	DC				2	Allele 1 (p.Q1513fs) was NGS-false-negative
39	c.4577C>T	p.T1526M	DC							1	

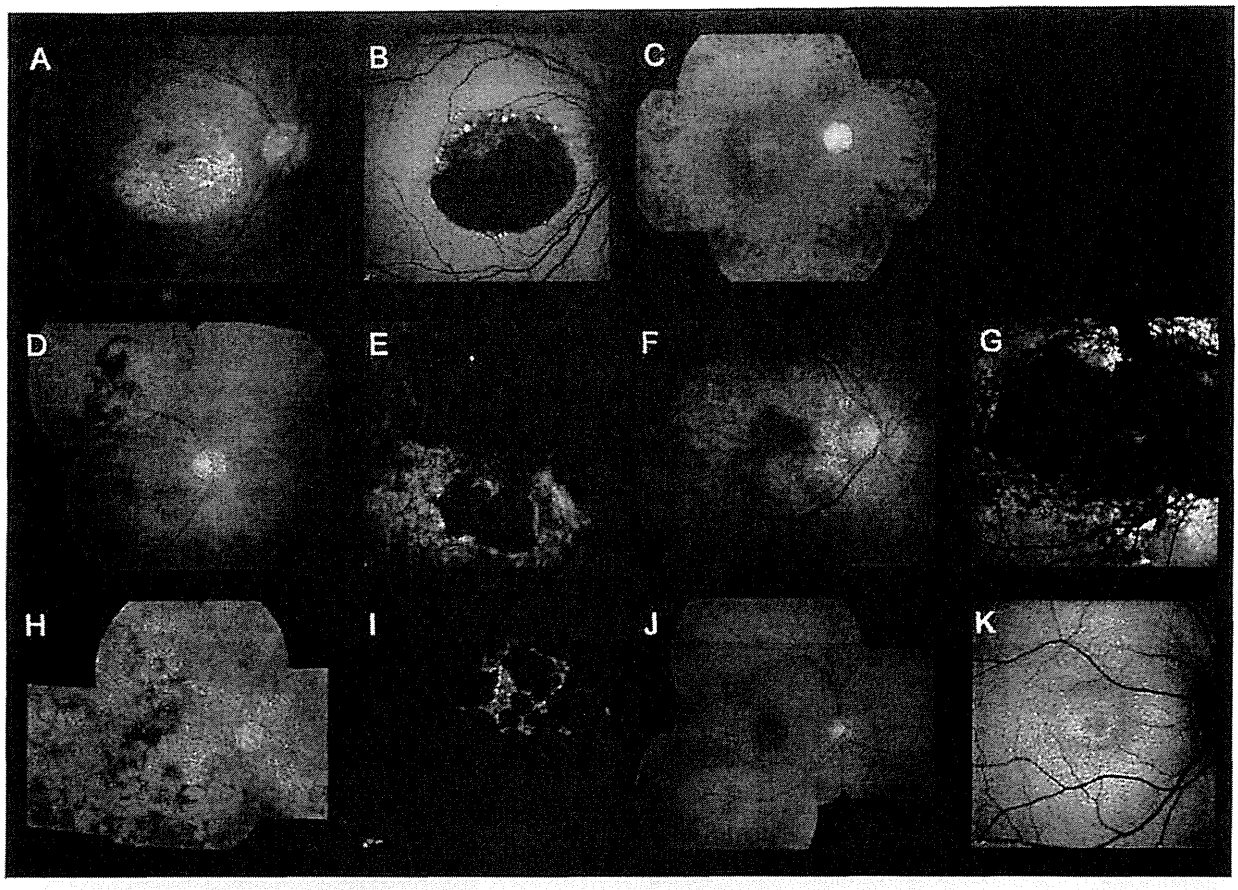

FIGURE 2. Color fundus photographs and autofluorescence images of six cases harboring a single, likely benign, missense variant with "atypical" clinical features for *ABCA4*-associated retinal disease (patients 74, 75, 76, 77, 78, and 79). Color photograph of patient 74 shows a geographic atrophy-like appearance (A), which on AF imaging is surrounded by foci of high and low AF signal (B). Patient 75 has evidence of generalized retinal atrophy in addition to marked macular atrophy, with dense pigmentation at the level of the RPE, and bone spicule formation, marked vessel attenuation, and optic disc pallor (C). Patient 76 has extensive macular atrophy extending beyond the arcades, with dense pigmentation at the level of the RPE and slight bone spicule pigmentation in the periphery (D). AF imaging demonstrates a heterogeneous background, but no peripapillary sparing (E). Patient 77 has a large area of macular atrophy extending to the optic disc (F), which on AF imaging is surrounded by an irregular low AF signal with foci of high and low signal, with no peripapillary sparing (G). Patient 78 has multiple widespread areas of atrophy with dense pigmentation at the level of RPE and bone spicule pigmentation in the periphery (H). AF imaging identifies multiple low signal areas with a heterogeneous background and no peripapillary sparing (I). Patient 79 has subtle atrophy confined to the fovea (J). AF imaging demonstrates a localized low AF signal at the fovea surrounded by a homogeneous background (K).

disease was calculated as the difference between age at onset and age at the latest examination.

Clinical Assessment

A full medical history was obtained and a comprehensive ophthalmologic examination was performed for all patients. Clinical assessment included best-corrected Snellen visual acuity (converted to equivalent logMAR visual acuity), fundus photography, autofluorescence (AF) imaging, spectral domain optical coherence tomography (SD-OCT), and electrophysiologic assessment.

Color fundus photography was performed with the TRC-50IA Retinal Fundus Camera (Topcon, Tokyo, Japan) and AF images were obtained using either an HRA 2 (excitation wavelength, 488 nm; barrier filter, 500 nm; field of view, 30 × 30°; Heidelberg Engineering, Heidelberg, Germany)[31] or Spectralis with viewing module version 5.1.2.0 (excitation wavelength, 488 nm; barrier filter, 500 nm; fields of view, 30 × 30° and 55 × 55°; Heidelberg Engineering) after pupillary dilation.[32] Patients were classified into one of three AF subtypes based on a recent report in *ABCA4*-associated retinal disease[31]: type 1—localized low AF signal at the fovea surrounded by a homogeneous background, type 2—localized low AF signal at the macula surrounded by a heterogeneous background, and type 3—multiple areas of low AF signal at the posterior pole with a heterogeneous background. SD-OCT imaging was obtained with the Spectralis with viewing module version 5.1.2.0.[32]

Electrophysiologic assessment included full-field electroretinography (ffERG) and pattern electroretinography (PERG) incorporating the standards of the International Society for Clinical Electrophysiology of Vision (ISCEV).[33,34] All components of the ffERG and PERG were taken into account when classifying patients into one of the three electrophysiologic groups:[4,35] group 1—patients with PERG P50 abnormality with normal ERGs, group 2—subjects with PERG P50 abnormality and additional generalized cone ERG abnormality (assessed with light adapted 30 Hz ERG and light adapted 3.0 ERG), and group 3—individuals with PERG P50 abnormality, and addi-

TABLE 1. Summary of Clinical Features of 79 Patients With *ABCA4*-Related Retinal Disease

Median age of onset, y (range)		22.0 (5–71)
Median age at examination, y (range)		40.0 (15–79)
Median duration of disease, y (range)		10.0 (0–54)
LogMAR visual acuity (range)	R	1.00 (−0.08–1.78)
	L	1.00 (−0.08–4.00)
AF subtype, $n = 71$	1	$n = 21$
	2	$n = 34$
	3	$n = 16$
ERG group, $n = 70$	1	$n = 34$
	2	$n = 7$
	3	$n = 29$

AF, autofluorescence; ERG, electroretinography; R, right eye; L, left eye.

novel NGS strategy for *ABCA4* screening in a large, well-characterized British cohort of patients with likely *ABCA4*-associated phenotypes and report novel disease-causing variants.

MATERIALS AND METHODS

Patients

Prescreening with APEX technology was performed in a cohort of 232 patients seen at Moorfields Eye Hospital with a clinical diagnosis of retinopathy compatible with *ABCA4*-associated retinal disease. Two or more variants were identified in 103 patients, one variant in 79 subjects, and no variants in 50 individuals. The 79 patients with only one *ABCA4* allele were recruited for this study. After informed consent was obtained, blood samples were taken from all individuals for NGS of *ABCA4*. The protocol of the study adhered to the provisions of the Declaration of Helsinki and was approved by the Ethics Committee of Moorfields Eye Hospital. The age at onset was defined as the age at which visual loss was first noted by the patient. The duration of

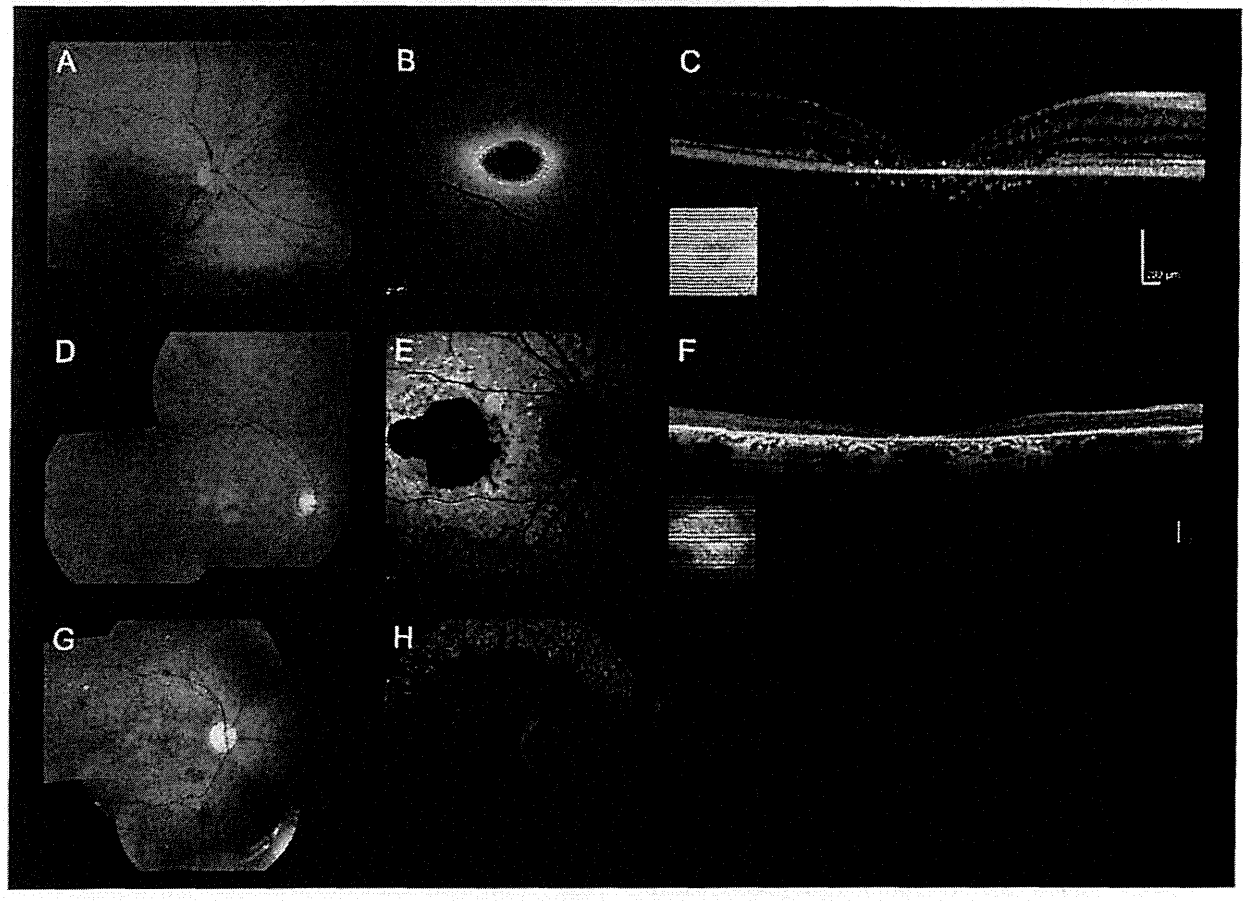

FIGURE 1. Color fundus photographs, autofluorescence images, and optical coherence tomography of three representative cases harboring two or more *ABCA4* variants with "typical" *ABCA4*-associated retinal disease (patients 19, 36, and 17). Color fundus photograph of patient 19 shows macular atrophy (**A**) and AF imaging demonstrates a localized low AF signal at the fovea, with a high signal edge surrounded by a homogeneous background (**B**). SD-OCT demonstrates marked outer retinal loss at the central macula (**C**). Patient 36 has macular atrophy surrounded by numerous yellow-white flecks (**D**) and a localized low AF signal at the macula surrounded by a heterogeneous background, with peripapillary sparing (**E**). Generalized loss of outer retinal architecture is seen on SD-OCT. Patient 17 has widespread multiple areas of atrophy with patchy pigmentation (**G**) and multiple areas of low AF signal at the posterior pole with a heterogeneous background (**H**).

ABCA4 Gene Screening by Next-Generation Sequencing in a British Cohort

Kaoru Fujinami,[1-4] Jana Zernant,[5] Ravinder K. Chana,[3,4] Genevieve A. Wright,[3,4] Kazushige Tsunoda,[1] Yoko Ozawa,[2] Kazuo Tsubota,[2] Andrew R. Webster,[3,4] Anthony T. Moore,[3,4] Rando Allikmets,[5,6] and Michel Michaelides[3,4]

[1]Laboratory of Visual Physiology, National Institute of Sensory Organs, National Tokyo Medical Center, Tokyo, Japan
[2]Department of Ophthalmology, Keio University, School of Medicine, Tokyo, Japan
[3]UCL Institute of Ophthalmology, London, United Kingdom
[4]Moorfields Eye Hospital, London, United Kingdom
[5]Department of Ophthalmology, Columbia University, New York, New York
[6]Department of Pathology and Cell Biology, Columbia University, New York, New York

Correspondence: Rando Allikmets, Columbia University, 630 West 168th Street, New York, NY 10032; rla22@columbia.edu.
Michel Michaelides, UCL Institute of Ophthalmology, 11-43 Bath Street, London, EC1V 9EL, UK; michel.michaelides@ucl.ac.uk.

Submitted: June 9, 2013
Accepted: August 19, 2013

Citation: Fujinami K, Zernant J, Chana RK, et al. *ABCA4* gene screening by next-generation sequencing in a British cohort. *Invest Ophthalmol Vis Sci.* 2013;54:6662-6674. DOI:10.1167/iovs.13-12570

PURPOSE. We applied a recently reported next-generation sequencing (NGS) strategy for screening the *ABCA4* gene in a British cohort with *ABCA4*-associated disease and report novel mutations.

METHODS. We identified 79 patients with a clinical diagnosis of *ABCA4*-associated disease who had a single variant identified by the *ABCA4* microarray. Comprehensive phenotypic data were obtained, and the NGS strategy was applied to identify the second allele by means of sequencing the entire coding region and adjacent intronic sequences of the *ABCA4* gene. Identified variants were confirmed by Sanger sequencing and assessed for pathogenicity by in silico analysis.

RESULTS. Of the 42 variants detected by prescreening with the microarray, in silico analysis suggested that 34, found in 66 subjects, were disease-causing and 8, found in 13 subjects, were benign variants. We detected 42 variants by NGS, of which 39 were classified as disease-causing. Of these 39 variants, 31 were novel, including 16 missense, 7 splice-site-altering, 4 nonsense, 1 in-frame deletion, and 3 frameshift variants. Two or more disease-causing variants were confirmed in 37 (47%) of 79 patients, one disease-causing variant in 36 (46%) subjects, and no disease-causing variant in 6 (7%) individuals.

CONCLUSIONS. Application of the NGS platform for *ABCA4* screening enabled detection of the second disease-associated allele in approximately half of the patients in a British cohort where one mutation had been detected with the arrayed primer extension (APEX) array. The time- and cost-efficient NGS strategy is useful in screening large cohorts, which will be increasingly valuable with the advent of *ABCA4*-directed therapies.

Keywords: ABCA4, next generation sequencing, Stargardt disease

Stargardt disease is the most common form of inherited macular dystrophy and is caused by recessive mutations in the *ABCA4* gene.[1,2] Stargardt disease typically presents with central macular atrophy and yellow-white flecks at the posterior pole, primarily at the level of the RPE.[2,3] A highly variable phenotype and progression of Stargardt disease have been documented, and mutations in *ABCA4* also have been implicated in cone dystrophy, cone-rod dystrophy, and "retinitis pigmentosa."[4-12] In this report, we will use the term "*ABCA4*-associated retinal disease" to refer to the broad range and variability of clinical manifestations of retinopathy due to *ABCA4* variants.

The carrier frequency of likely pathogenic *ABCA4* alleles has been reported to be as high as 1:20[13,14] and more than 700 *ABCA4* variants have been identified so far.[1,2,5-29] The high allelic heterogeneity makes molecular genetic analyses of *ABCA4*-associated retinal disease very challenging. It has been reported that direct Sanger sequencing of the entire *ABCA4* coding region (50 exons) detects between 66% and 80% of disease-causing alleles[13,21]; however, this approach has significant limitations in large patient cohorts due to the prohibitive time and cost implications.[3,5]

Since the development of the *ABCA4* genotyping microarray, using arrayed primer extension (APEX) technology,[14] systematic screening of all known previously reported *ABCA4* variants has been available[26,30]; APEX detects approximately 65% to 75% of all disease-associated alleles. However, by definition, novel variants are not detected by APEX technology, necessitating the use of other methodologies for high-throughput systematic screening of the entire coding region, especially in cases where one or both disease-causing alleles have failed to be identified by the array.

Zernant et al. recently reported the capability of a next-generation sequencing (NGS) strategy to detect new *ABCA4* variants that were not included on the APEX array; all 50 *ABCA4* exons of 168 patients were amplified in parallel using an amplicon tagging PCR protocol and NGS was applied to the resulting amplicons.[5] The purpose of this study was to apply this

22. Maeda T, Maeda A, Matosky M, et al. Evaluation of potential therapies for a mouse model of human age-related macular degeneration caused by delayed all-trans-retinal clearance. *Invest Ophthalmol Vis Sci*. 2009;50:4917–4925.
23. Okano K, Maeda A, Chen Y, et al. Retinal cone and rod photoreceptor cells exhibit differential susceptibility to light-induced damage. *J Neurochem*. 2012;121:146–156.
24. Chen Y, Okano K, Maeda T, et al. Mechanism of all-trans-retinal toxicity with implications for Stargardt disease and age-related macular degeneration. *J Biol Chem*. 2012;287:5059–5069.
25. Mata NL, Weng J, Travis GH. Biosynthesis of a major lipofuscin fluorophore in mice and humans with ABCR-mediated retinal and macular degeneration. *Proc Natl Acad Sci U S A*. 2000;97:7154–7159.
26. Sparrow JR, Gregory-Roberts E, Yamamoto K, et al. The bisretinoids of retinal pigment epithelium. *Prog Retin Eye Res*. 2012;31:121–135.
27. Sparrow JR, Nakanishi K, Parish CA. The lipofuscin fluorophore A2E mediates blue light-induced damage to retinal pigmented epithelial cells. *Invest Ophthalmol Vis Sci*. 2000;41:1981–1989.
28. Dorey CK, Wu G, Ebenstein D, Garsd A, Weiter JJ. Cell loss in the aging retina. Relationship to lipofuscin accumulation and macular degeneration. *Invest Ophthalmol Vis Sci*. 1989;30:1691–1699.
29. von Ruckmann A, Fitzke FW, Bird AC. Distribution of fundus autofluorescence with a scanning laser ophthalmoscope. *Br J Ophthalmol*. 1995;79:407–412.
30. Chen B, Tosha C, Gorin MB, Nusinowitz S. Analysis of autofluorescent retinal images and measurement of atrophic lesion growth in Stargardt disease. *Exp Eye Res*. 2010;91:143–152.
31. Fishman GA, Stone EM, Grover S, Derlacki DJ, Haines HL, Hockey RR. Variation of clinical expression in patients with Stargardt dystrophy and sequence variations in the ABCR gene. *Arch Ophthalmol*. 1999;117:504–510.
32. Burke TR, Tsang SH. Allelic and phenotypic heterogeneity in ABCA4 mutations. *Ophthalmic Genet*. 2011;32:165–174.
33. Zernant J, Schubert C, Im KM, et al. Analysis of the ABCA4 gene by next-generation sequencing. *Invest Ophthalmol Vis Sci*. 2011;52:8479–8487.
34. Allikmets R. A photoreceptor cell-specific ATP-binding transporter gene (ABCR) is mutated in recessive Stargardt macular dystrophy. *Nat Genet*. 1997;17:122.
35. Rozet JM, Gerber S, Souied E, et al. Spectrum of ABCR gene mutations in autosomal recessive macular dystrophies. *Eur J Hum Genet*. 1998;6:291–295.
36. Lewis RA, Shroyer NF, Singh N, et al. Genotype/phenotype analysis of a photoreceptor-specific ATP-binding cassette transporter gene, ABCR, in Stargardt disease. *Am J Hum Genet*. 1999;64:422–434.
37. Maugeri A, Klevering BJ, Rohrschneider K, et al. Mutations in the ABCA4 (ABCR) gene are the major cause of autosomal recessive cone-rod dystrophy. *Am J Hum Genet*. 2000;67:960–966.
38. Papaioannou M, Ocaka L, Bessant D, et al. An analysis of ABCR mutations in British patients with recessive retinal dystrophies. *Invest Ophthalmol Vis Sci*. 2000;41:16–19.
39. Rivera A, White K, Stohr H, et al. A comprehensive survey of sequence variation in the ABCA4 (ABCR) gene in Stargardt disease and age-related macular degeneration. *Am J Hum Genet*. 2000;67:800–813.
40. Birch DG, Peters AY, Locke KL, Spencer R, Megarity CF, Travis GH. Visual function in patients with cone-rod dystrophy (CRD) associated with mutations in the ABCA4(ABCR) gene. *Exp Eye Res*. 2001;73:877–886.
41. Briggs CE, Rucinski D, Rosenfeld PJ, Hirose T, Berson EL, Dryja TP. Mutations in ABCR (ABCA4) in patients with Stargardt macular degeneration or cone-rod degeneration. *Invest Ophthalmol Vis Sci*. 2001;42:2229–2236.
42. Fumagalli A, Ferrari M, Soriani N, et al. Mutational scanning of the ABCR gene with double-gradient denaturing-gradient gel electrophoresis (DG-DGGE) in Italian Stargardt disease patients. *Hum Genet*. 2001;109:326–338.
43. Shroyer NF, Lewis RA, Yatsenko AN, Wensel TG, Lupski JR. Cosegregation and functional analysis of mutant ABCR (ABCA4) alleles in families that manifest Stargardt disease and age-related macular degeneration. *Hum Mol Genet*. 2001;10:2671–2678.
44. Webster AR, Heon E, Lotery AJ, et al. An analysis of allelic variation in the ABCA4 gene. *Invest Ophthalmol Vis Sci*. 2001;42:1179–1189.
45. Lange C, Feltgen N, Junker B, Schulze-Bonsel K, Bach M. Resolving the clinical acuity categories "hand motion" and "counting fingers" using the Freiburg Visual Acuity Test (FrACT). *Graefes Arch Clin Exp Ophthalmol*. 2009;247:137–142.
46. Robson AG, Tufail A, Fitzke F, et al. Serial imaging and structure-function correlates of high-density rings of fundus autofluorescence in retinitis pigmentosa. *Retina*. 2011;31:1670–1679.
47. Bellmann C, Rubin GS, Kabanarou SA, Bird AC, Fitzke FW. Fundus autofluorescence imaging compared to different confocal scanning laser ophthalmoscopes. *Br J Ophthalmol*. 2003;87:1381–1386.
48. Robson AG, Egan CA, Luong VA, Bird AC, Holder GE, Fitzke FW. Comparison of fundus autofluorescence with photopic and scotopic fine-matrix mapping in patients with retinitis pigmentosa and normal visual acuity. *Invest Ophthalmol Vis Sci*. 2004;45:4119–4125.
49. Sergouniotis PI, Davidson AE, Lenassi E, Devery SR, Moore AT, Webster AR. Retinal structure, function, and molecular pathologic features in gyrate atrophy. *Ophthalmology*. 2012;119:596–605.
50. Orita M, Iwahana H, Kanazawa H, Hayashi K, Sekiya T. Detection of polymorphisms of human DNA by gel electrophoresis as single-strand conformation polymorphisms. *Proc Natl Acad Sci U S A*. 1989;86:2766–2770.
51. Jaakson K, Zernant J, Kulm M, et al. Genotyping microarray (gene chip) for the ABCR (ABCA4) gene. *Hum Mutat*. 2003;22:395–403.
52. Ng PC, Henikoff S. SIFT: predicting amino acid changes that affect protein function. *Nucleic Acids Res*. 2003;31:3812–3814.
53. Adzhubei IA, Schmidt S, Peshkin L, et al. A method and server for predicting damaging missense mutations. *Nat Methods*. 2010;7:248–249.
54. Sodi A, Bini A, Passerini I, Forconi S, Menchini U, Torricelli F. Different patterns of fundus autofluorescence related to ABCA4 gene mutations in Stargardt disease. *Ophthalmic Surg Lasers Imaging*. 2010;41:48–53.
55. Klevering BJ, Yzer S, Rohrschneider K, et al. Microarray-based mutation analysis of the ABCA4 (ABCR) gene in autosomal recessive cone-rod dystrophy and retinitis pigmentosa. *Eur J Hum Genet*. 2004;12:1024–1032.
56. Schindler EI, Nylen EL, Ko AC, et al. Deducing the pathogenic contribution of recessive ABCA4 alleles in an outbred population. *Hum Mol Genet*. 2010;19:3693–3701.
57. Cella W, Greenstein VC, Zernant-Rajang J, et al. G1961E mutant allele in the Stargardt disease gene ABCA4 causes bull's eye maculopathy. *Exp Eye Res*. 2009;89:16–24.
58. Fujinami K, Zernant J, Chana RK, et al. ABCA4 gene screening by next-generation sequencing in a British cohort. *Invest Ophthalmol Vis Sci*. 2013;54:6662–6674.

agreement in atrophy measurement. Software, which defines and calculates the atrophic lesions automatically, may arguably be more reliable in performing quantitative analysis, although this also is not without its limitations. Many of the older AF images at baseline in our study could not be analyzed with such recent software. Quantitative analysis of optical coherence tomography data also will have an important role in future studies of atrophy progression. In addition, wide-field AF imaging systems also may aid a more comprehensive assessment in terms of AF type classification (less atrophic lesions "beyond the scope" of the acquired image) and quantitative atrophy measurement.

Two different gene screening methods (SSCP and microarray) were applied in our cohort due to the technological advances made during the period of this study. In keeping with previous studies, we were able to undertake segregation analysis in a limited number of cases due to the unavailability of other family samples. Undoubtedly, more advanced recent mutation analysis, such as PCR enrichment-based next-generation sequencing (NGS), will result in a higher mutation detection rate, including identifying the often "missing" second *ABCA4* allele, which will allow more informed genotype-phenotype correlations to be investigated.[33,58] The genotype-phenotype correlations have been investigated by comparing the *ABCA4* gene mutations with the clinical features in this study; however, it is likely that other factors must be considered, including environmental, genetic, and epigenetic modifiers.

This study has investigated AF subtypes/patterns in a longitudinal survey, and determined changes in AF pattern and progression of atrophy. It has highlighted that patients with localized foveal atrophy tend to experience milder progression, including milder visual acuity loss, whereas those subjects with multiple large areas of retinal atrophy had severe progression and severe visual acuity reduction. These data assist counselling with regard to visual prognosis, and may help in study design and patient selection of clinical trials for *ABCA4*-related retinopathy.

Acknowledgments

The authors thank Graham E. Holder, Antony G. Robson, Alice E. Davidson, Panagiotis I. Sergouniotis, Arundhati Dev Borman, Eva Lenassi, Naushin Waseem, Bev Scott, Genevieve Wright, Sophie Devery, and Ravinder Chana (UCL Institute of Ophthalmology, London, United Kingdom), and Yozo Miyake (Aichi Medical University, Aichi, Japan), for their contribution to this study.

Supported by grants from the National Institute for Health Research Biomedical Research Center at Moorfields Eye Hospital National Health Service Foundation Trust and UCL Institute of Ophthalmology (United Kingdom), Fight For Sight (United Kingdom), Moorfields Eye Hospital Special Trustees (United Kingdom), Macular Disease Society (United Kingdom), the Foundation Fighting Blindness (United States), Suzuken Memorial Foundation (Japan), Mitsukoshi Health and Welfare Foundation (Japan), and Daiwa Anglo-Japanese Foundation (Japan), and by an FFB Career Development Award (MM). The authors alone are responsible for the content and writing of the paper.

Disclosure: **K. Fujinami**, None; **N. Lois**, None; **R. Mukherjee**, None; **V.A. McBain**, None; **K. Tsunoda**, None; **K. Tsubota**, None; **E.M. Stone**, None; **F.W. Fitzke**, None; **C. Bunce**, None; **A.T. Moore**, None; **A.R. Webster**, None; **M. Michaelides**, None

References

1. Michaelides M, Hunt DM, Moore AT. The genetics of inherited macular dystrophies. *J Med Genet*. 2003;40:641–650.
2. Michaelides M, Chen LL, Brantley MA Jr, et al. ABCA4 mutations and discordant ABCA4 alleles in patients and siblings with bull's-eye maculopathy. *Br J Ophthalmol*. 2007; 91:1650–1655.
3. Lois N, Holder GE, Fitzke FW, Plant C, Bird AC. Intrafamilial variation of phenotype in Stargardt macular dystrophy—fundus flavimaculatus. *Invest Ophthalmol Vis Sci*. 1999;40: 2668–2675.
4. Lois N, Holder GE, Bunce C, Fitzke FW, Bird AC. Phenotypic subtypes of Stargardt macular dystrophy—fundus flavimaculatus. *Arch Ophthalmol*. 2001;119:359–369.
5. Lois N, Halfyard AS, Bird AC, Holder GE, Fitzke FW. Fundus autofluorescence in Stargardt macular dystrophy—fundus flavimaculatus. *Am J Ophthalmol*. 2004;138:55–63.
6. McBain VA, Townend J, Lois N. Progression of retinal pigment epithelial atrophy in Stargardt disease. *Am J Ophthalmol*. 2012;154:146–154.
7. Aaberg TM. Stargardt's disease and fundus flavimaculatus: evaluation of morphologic progression and intrafamilial coexistence. *Trans Am Ophthalmol Soc*. 1986;84:453–487.
8. Armstrong JD, Meyer D, Xu S, Elfervig JL. Long-term follow-up of Stargardt's disease and fundus flavimaculatus. *Ophthalmology*. 1998;105:448–457, discussion 457–448.
9. Fujinami K, Lois N, Davidson AE, et al. A longitudinal study of Stargardt disease: clinical and electrophysiologic assessment, progression, and genotype correlations. *Am J Ophthalmol*. 2013;155:1075–1088.
10. Fujinami K, Sergouniotis PI, Davidson AE, et al. The clinical effect of homozygous ABCA4 alleles in 18 patients. *Ophthalmology*. 2013;120:2324–2331.
11. Fujinami K, Akahori M, Fukui M, Tsunoda K, Iwata T, Miyake Y. Stargardt disease with preserved central vision: identification of a putative novel mutation in ATP-binding cassette transporter gene. *Acta Ophthalmol*. 2011;89:e297–e298.
12. Fujinami K, Sergouniotis PI, Davidson AE, et al. Clinical and molecular analysis of Stargardt disease with preserved foveal structure and function. *Am J Ophthalmol*. 2013;156:487–501.
13. Allikmets R, Shroyer NF, Singh N, et al. Mutation of the Stargardt disease gene (ABCR) in age-related macular degeneration. *Science*. 1997;277:1805–1807.
14. Allikmets R, Singh N, Sun H, et al. A photoreceptor cell-specific ATP-binding transporter gene (ABCR) is mutated in recessive Stargardt macular dystrophy. *Nat Genet*. 1997;15: 236–246.
15. Cremers FP, van de Pol DJ, van Driel M, et al. Autosomal recessive retinitis pigmentosa and cone-rod dystrophy caused by splice site mutations in the Stargardt's disease gene ABCR. *Hum Mol Genet*. 1998;7:355–362.
16. Martinez-Mir A, Paloma E, Allikmets R, et al. Retinitis pigmentosa caused by a homozygous mutation in the Stargardt disease gene ABCR. *Nat Genet*. 1998;18:11–12.
17. Fishman GA, Stone EM, Eliason DA, Taylor CM, Lindeman M, Derlacki DJ. ABCA4 gene sequence variations in patients with autosomal recessive cone-rod dystrophy. *Arch Ophthalmol*. 2003;121:851–855.
18. Sun H, Nathans J. Stargardt's ABCR is localized to the disc membrane of retinal rod outer segments. *Nat Genet*. 1997;17: 15–16.
19. Weng J, Mata NL, Azarian SM, Tzekov RT, Birch DG, Travis GH. Insights into the function of Rim protein in photoreceptors and etiology of Stargardt's disease from the phenotype in abcr knockout mice. *Cell*. 1999;98:13–23.
20. Molday LL, Rabin AR, Molday RS. ABCR expression in foveal cone photoreceptors and its role in Stargardt macular dystrophy. *Nat Genet*. 2000;25:257–258.
21. Maeda A, Maeda T, Golczak M, Palczewski K. Retinopathy in mice induced by disrupted all-trans-retinal clearance. *J Biol Chem*. 2008;283:26684–26693.

TABLE 4. Association Between AF Subtype and Genotype in 26 Patients With Two or More Disease-Causing *ABCA4* Variants

	Patients Harboring at Least One Null Variant, $n = 14$		Patients Harboring Two or More Missense Variants, $n = 12$	
	BL	FU	BL	FU
AF type 1	3 (2)	1	5 (2)	3
AF type 2	8 (2)	8	7 (1)	8
AF type 3	3	5	0	1
Total, $n = 26$	14	14	12	12

One patient harboring null variants was excluded from this analysis due to an asymmetric AF subtype at baseline (patient 61). The number of patients who showed AF subtype transition is shown in parentheses.

disease, baseline logMAR visual acuity, and logMAR visual acuity reduction. Patients with type 1 AF at baseline had a later onset of central visual loss and better visual acuity, compared to patients with type 3 AF at baseline. Correlation between duration of disease and size of atrophy, and duration of disease and RAE also were established; thereby supporting the recent suggestion that a longer disease duration is associated with more extensive and more rapidly progressive central retinal atrophy.[30]

Overall, the findings of this study suggested that patients with Stargardt disease showing localized foveal atrophy have milder progression of central atrophy compared to subjects with multiple atrophic lesions who have more rapid loss of central retinal structure over time. In contrast, patients in the "intermediate" group, with macular atrophy and a heterogeneous background, have a more variable area of atrophy and atrophy enlargement. An association between the pattern of functional loss detected on electrophysiology and the RAE was suggested in previous reports[6,30]; therefore, electrophysiological assessment may assist in the characterization of patients with an "intermediate" phenotype. Furthermore a comprehensive study of the relationship over a long-term follow-up period between AF and electrophysiology in a larger cohort of patients with Stargardt disease would be valuable.

We identified 45 likely disease-causing *ABCA4* variants, with two putative novel mutations detected. A total of 26 patients harbored two or more likely disease-causing variants; there was a statistically significant association between AF subtype classification and genotype group classification at baseline and follow-up. A difference was suggested between genotype groups in terms of proportion of AF subtypes 1 and 3, in keeping with more deleterious genetic variants being associated with a more severe and progressive AF phenotype. Sodi et al.,[54] in an AF study of 20 patients, also concluded that the presence of two severe mutations was associated with a larger area of macular atrophy.

Consistent with previous reports, four of nine patients with the c.5461-10 T>C variant had a severe phenotype, with multiple large areas of atrophy.[9,33,55,56] In contrast, there were three patients with the c.5461-10 T>C variant with a lower atrophy enlargement, all of whom also harbored missense variants (p.Gly1961Glu in one patient, and p.Leu2027Phe in the remaining two subjects); considered to be associated with a milder phenotype.[2,10,54,56,57] The substitutions p.Leu2027-Phe, and to a greater extent p.Gly1961Glu, also were associated with a milder AF phenotype in our study. Larger numbers of patients are needed to investigate the phenotypic characteristics of other rare alleles.

There are several potential limitations of this study, many of which are inherent to retrospective studies, including study population selection, the variable number and interval of examinations during follow-up, the definition of atrophic lesions on AF images, AF subtype classification, and the strategy of mutation screening and genotype grouping. Of the recruited patients, 62% at baseline and 54% at follow-up were in AF subtype 2, with the number of patients with AF subtype 3 being relatively small; a larger prospective cohort will be helpful to gain an improved understanding of the pathophysiological features associated with AF subtype 3 and also address many of the aforementioned limitations of retrospective studies.

This study was designed to observe the progression between the two time points (baseline and follow-up) and the assumption of linear progression was made for atrophy enlargement in keeping with previous reports.[6,30] This study has not examined the linearity of change between baseline and follow-up testing; a prospective study with additional more frequent time point sampling will help address this pertinent question. It is possible that progression will be linear in some individuals and nonlinear in others, in keeping with the commonplace phenotypic heterogeneity of inherited retinal disorders.

The definition of the significant low gray scale on AF images can be challenging—nevertheless it is very reassuring that the two investigators in this study showed statistically significant

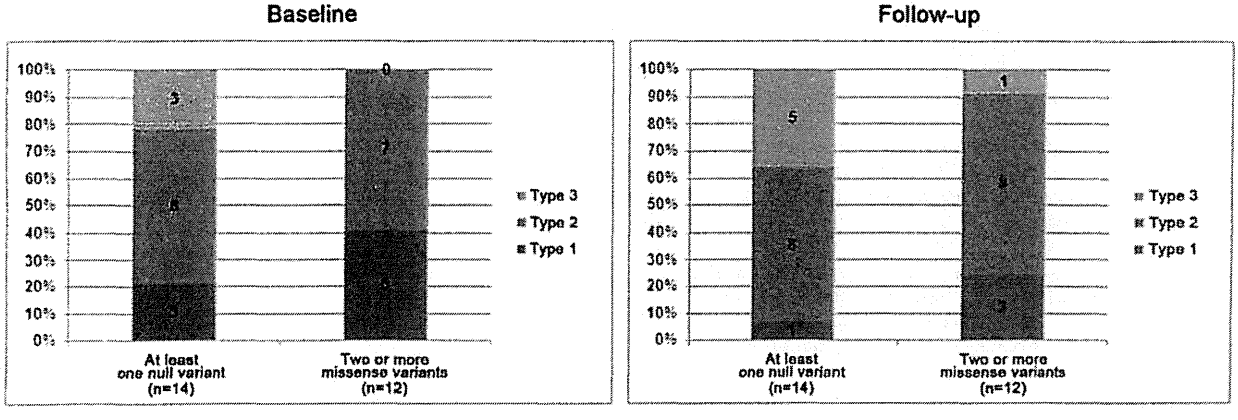

FIGURE 5. The association between genotype group and AF type at baseline and follow-up. The proportion of each AF subtype for each genotype group is shown in the *bar graphs*. In 26 patients with two or more likely disease-causing variants, there was a statistically significant association between AF subtype classification and genotype group classification at baseline and follow-up.

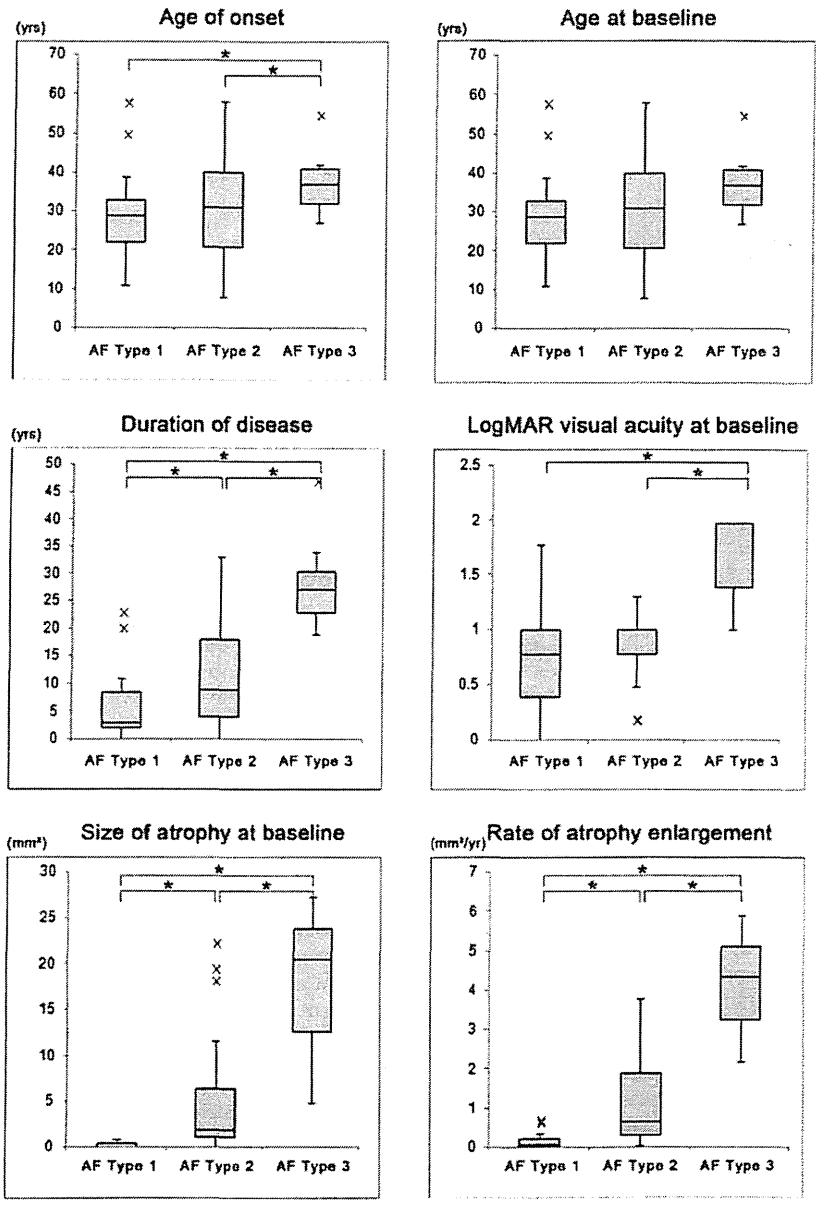

FIGURE 4. A comparison of selected clinical features and quantitative AF imaging data associated with each AF subtype at baseline in 67 patients with Stargardt disease, showing significant differences in age of onset, duration of disease, visual acuity at baseline, size of atrophy at baseline, and rate of atrophy enlargement. The *boxes* show the median, and 25% and 75% confidence interval (lower and upper quartiles). The *whiskers* extend to what could be considered the 95% confidence interval. *Crosses* represent values outside the 95% confidence interval. *Statistically significant differences.

may inform patient selection for future therapeutic interventions for *ABCA4*-related retinopathy.

We classified patients into three AF subtypes at baseline. Of patients with type 1 AF at baseline, 58% remained in type 1 AF at follow-up, whereas 12% of patients with type 2 AF showed transition to type 3 AF. Type 3 appears to be a comparatively distinct phenotype, given the fact that only a relatively small number of subjects had progression from AF type 2 to type 3, and none of the type 1 AF patients showed transition to type 3 AF. Statistically significant differences between baseline AF types in RAE also were demonstrated, suggesting a less severe and more slowly progressive phenotype in type 1 AF, and more severe and more rapid enlargement of atrophy in type 3 AF. The correlation between the total size of atrophy and RAE also supports this proposal.

There was one patient (patient 61) with an asymmetric AF subtype at baseline, type 3 in the right eye and type 2 in the left, with type 3 in both eyes at follow-up. Many possible factors may have a role in interocular asymmetry, including anisometropia, skewed X-inactivation of a modifier (in females), differences in mitochondrial sequences, somatic mutation, epigenetic differences, and "stochastic" factors (e.g., small initial differences in gene expression leading to significant differences later).

The clinical characteristics of each AF subtype showed significant differences in terms of age of onset, duration of

TABLE 3. Clinical Features and Quantitative AF Data Associated With AF Subtype at Baseline in 67 Patients With Stargardt Disease

	Median Age of Onset, y	Median Duration, y	Median Age, y		Mean Interval, y	LogMAR Visual Acuity			Median Size of Atrophy, mm²		Rate of Atrophy Enlargement, mm²/y
			BL	FU		BL	FU	Reduction	BL	FU	
Type 1, $n = 19$	24.0	3.0	29.0	36.0	9.2	0.78	1.00	0.22	0.00	1.00	0.06
Type 2, $n = 41$	18.0	9.0	31.0	38.0	9.0	1.00	1.00	0.22	1.91	8.52	0.67
Type 3, $n = 7$	8.0	27.0	37.0	43.0	9.1	1.98	1.78	0.00	20.54	57.17	4.37
Total, $n = 67$	19.0	9.0	31.0	39.0	9.1	1.00	1.00	0.12	1.12	5.32	0.45

One patient was excluded from baseline AF subtype analysis due to an asymmetric AF subtype at baseline (patient 61). The age of onset was defined as the age at which visual loss was first noted by the patient. The duration of disease was calculated as the difference between age at onset and age at the baseline examination when AF imaging was obtained. The interval of observation was determined by the difference between the age at baseline and the age at the most recent "follow-up" examination at which AF imaging was obtained. The rate of atrophy enlargement (mm²/y) was calculated as follows: size of the area of atrophy at last follow-up minus size of the area of atrophy at baseline (mm²) divided by the follow-up time (years). BL, baseline; FU, follow-up.

atrophy and median RAE associated with each baseline AF subtype are shown in Table 3 and Figure 4. There was a statistically significant difference between AF type 1 and 3, and type 2 and 3 in terms of age of onset ($P = 0.003$ and 0.016, respectively). In respect to duration of disease, there were statistically significant differences between AF types 1 and 2, types 1 and 3, and types 2 and 3 ($P = 0.018$, 0.002, and 0.001, respectively). There also was a statistically significant difference in logMAR visual acuity at baseline between AF types 1 and 3, and types 2 and 3 ($P = 0.003$ and 0.003, respectively), and in logMAR visual acuity reduction between types 1 and 3, and types 2 and 3 ($P = 0.042$ and 0.008, respectively). With respect to size of atrophy at baseline and RAE, statistically significant differences were seen between types 1 and 2, types 1 and 3, and types 2 and 3 ($P = 0.000$, $P = 0.049$, $P = 0.000$ for size of atrophy at baseline, and $P = 0.000$, $P = 0.019$, 0.014 for RAE, respectively). However, there were no statistically significant differences between AF subtypes in terms of other parameters, including age at baseline and follow-up interval.

The Spearman rank correlation test was applied for assessment of the relationships between parameters, including age of onset and size of atrophy at baseline, age at baseline and size of atrophy at baseline, duration of disease and size of atrophy at baseline, age of onset and RAE, age at baseline and RAE, duration of disease and RAE, and size of atrophy at baseline and RAE. There was a statistically significant correlation between age at baseline and size of atrophy at baseline ($\rho = 0.402$, $P < 0.0015$), duration of disease and size of atrophy at baseline ($\rho = 0.626$, $P < 0.0001$), age at baseline and RAE ($\rho = 0.369$, $P < 0.0037$), duration of disease and RAE ($\rho = 0.607$, $P < 0.0001$), and size of atrophy at baseline and RAE ($\rho = 0.767$, $P < 0.0001$). A tendency of negative correlation also was suggested between age of onset and RAE ($\rho = -0.191$, $P = 0.133$).

Molecular Genetics

Likely disease-causing variants in *ABCA4* were detected in 57 of 68 patients; with two or more variants identified in 27 patients and one variant in 30 subjects (Supplementary Table S1). Detailed results including in silico analysis are shown in Supplementary Table S2. A total of 45 variants was found in 57 patients; 13 null mutations, including one disease-associated intronic change and one predicted to affect splicing; and 32 missense variants. A total of 22 patients harbored at least one null variant, with a single subject having two null mutations. Of these 45 variants 43 have been reported previously and 2 are putative novel mutations: c.93G>A, p.Tyr31* and c.617_618delCG, p.Ser206Argfs*320 (Supplementary Tables S1, S2). The 26 patients harboring two or more disease-causing variants were classified into two genotype groups (Table 4); there were 14 patients with at least one null variant and 12 with two or more missense variants.

Genotype–AF Phenotype Correlations

The association between AF subtype and genotype group is shown in Table 4 and Figure 5. In 26 patients with two or more likely disease-causing variants, there was a statistically significant association between AF subtype classification and genotype group classification at baseline and follow-up ($\gamma = -0.567$ and $\gamma = -0.646$, respectively). There was a suggestion of a difference between the two genotype groups, in terms of proportion of AF subtypes 1 and 3. The proportion of AF subtype 1 was 21% at baseline and 7% at follow-up for the null variant genotype group, compared to 36% at baseline and 25% at follow-up for the missense variant genotype group. The proportion of AF subtype 3 was 21% and 36% at baseline and follow-up for the null variant genotype group, compared to 0% and 8% at baseline and follow-up, respectively, for the missense variant genotype group.

Four of nine patients from eight families harboring the variant c.5461-10 T>C were classified into type 3 AF at baseline and three (including one sibling pair) of these subjects had atrophy that extended beyond the limits of the AF image obtained (Supplementary Table S1). The median size of atrophy at baseline and follow-up in the remaining six patients was 0.92 and 6.29 mm², respectively. The median RAE of these patients harboring the variant c.5461-10 T>C was 0.45 mm²/y.

Four of eight patients from eight families harboring the missense variant p.Leu2027Phe had small central atrophy (<0.18 mm²) at baseline (Supplementary Table S1). The median size of atrophy at baseline and median RAE of these eight patients was 0.27 mm² and 0.39 mm²/y, respectively, which are less than the median values for the entire cohort of 68 patients (1.12 mm² and 0.45 mm²/y). The median size of atrophy at baseline and the median RAE of the five patients from five families harboring the missense variant p.Gly1961Glu also was relatively small; 0.47 mm² and 0.20 mm²/y respectively (Supplementary Table S1).

DISCUSSION

This study assessed longitudinal changes in RPE atrophy by undertaking AF imaging in a large well-characterized cohort of patients with Stargardt disease; 84% of subjects harbored at least one likely disease-causing *ABCA4* allele. The findings herein assist in providing improved advice on prognosis and

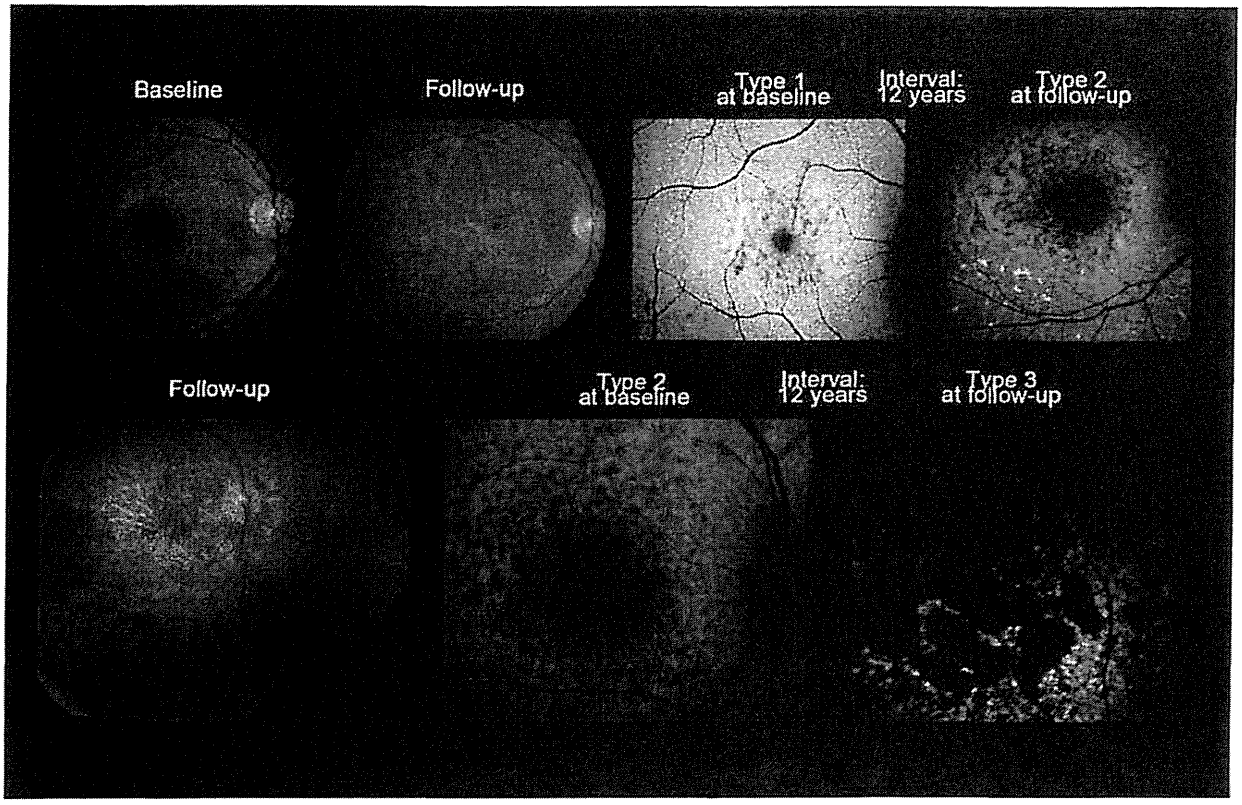

FIGURE 3. Color fundus photographs and AF images of two representative cases with Stargardt disease, showing AF subtype transition over time (patients 12 and 59). *Top row*: Color fundus photographs of patient 12 showing mild foveal atrophy surrounded by parafoveal yellowish-white flecks at baseline and more marked macular atrophy surrounded by numerous atrophic flecks extending anterior to the vascular arcades at follow-up. AF imaging demonstrates localized low signal at the fovea surrounded by a homogeneous background with high and low signal parafoveal foci at baseline, and a macular low signal lesion surrounded by numerous high and low signal foci throughout the posterior pole with a heterogeneous background at follow-up, consistent with transition from AF type 1 to type 2. *Bottom row*: Patient 59 had extensive areas of atrophy extending beyond the vascular arcades with atrophic flecks at follow-up. AF imaging showed subtype transition; a mottled macular low signal lesion surrounded by numerous low signal foci with a heterogeneous background (type 2) at baseline, and multiple areas of low signal throughout the posterior pole with a heterogeneous background (type 3) at follow-up. The central atrophy at follow-up extended beyond the limits of the AF image ("beyond the scope").

(patients 11, 31, 36, 39, 44, 56) had unavailable AF images at baseline of the left eye.

At baseline, 67 patients were classified based on the AF findings into three subtypes: 19 patients (28%) in type 1, 41 (61%) in type 2, and 7 (10%) in type 3. At follow-up there were 11 (16%) in type 1, 44 (66%) in type 2, and 12 (18%) in type 3 (Table 2). All patients had a symmetrical AF subtype between eyes, except for patient 61 with type 3 in the right and type 2 in the left at baseline, with type 3 chosen as the overall classification for this patient.

A total of 13 patients (28%) showed AF subtype transition during follow-up; 8/19 (42%) subjects from AF type 1 to AF type 2, and 5/41 (12%) individuals from AF type 2 to AF type 3 (Table 2). Three of five sibships were concordant for AF subtype at baseline (patients 31 and 37; 35 and 36; and 63 and 64) and two of five were discordant (patients 13 and 23; and 18 and 23); all the sibships were concordant at follow-up (Supplementary Table S1).

A total of 13 patients (19%) at baseline and 2 (2%) at follow-up had a single small area of low signal (<0.18 mm^2) in the selected eye and were recorded as having zero mm^2 of atrophy (Supplementary Table S1). There were six patients who had atrophy in the selected eye extending beyond the limits of the AF image at baseline and, thereby, they were excluded from the quantitative analyses (Supplementary Table S1). The median total size of atrophy at baseline and follow-up was 1.12 mm^2 (range, 0.00–27.23) and 5.32 mm^2 (range, 0.00–62.58), respectively. The median RAE over time was 0.45 mm^2/y (range, 0.00–5.89). The concordance correlation coefficient revealed significant agreement between the two observers' measurements (concordance correlation coefficient was 0.99). The clinical features of each baseline AF subtype are summarized in Table 3 and Figure 4. The median size of

TABLE 2. Distribution and Transition of AF Subtypes of 67 Patients With Stargardt Disease

	AF Type at Follow-up		
	Type 1	Type 2	Type 3
AF type at baseline			
Type 1, $n = 19$	11	8	0
Type 2, $n = 41$		36	5
Type 3, $n = 7$			7
Total, $n = 67$	11	44	12

One patient was excluded for this analysis due to an asymmetric AF subtype at baseline (patient 61).

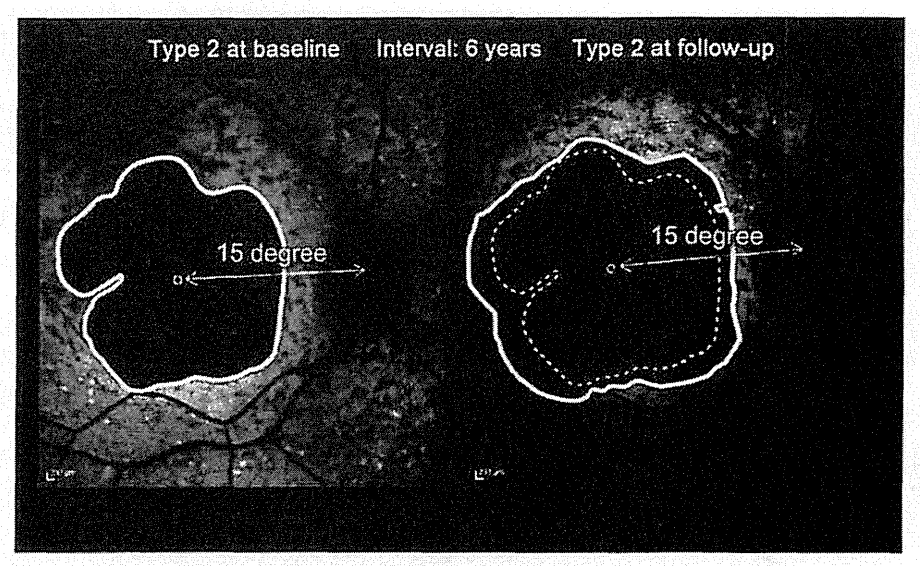

FIGURE 2. Measurement of the low signal area of AF and calculation of the rate of atrophy enlargement in a representative case with Stargardt disease. The area of low AF signal (patient 51) was measured using custom software, which enables measurement of the dimensions of the area outlined manually (*white line* in the *left* and *right* images) and the automatic computation of the area expressed in square degrees to facilitate the appreciation of the relation to the patient's visual function; with a given distance between the center of the optic nerve head and the foveola defined as 15° (marked in the images). Atrophy enlargement over time was calculated as the difference between the size of atrophy at baseline and follow-up (*broken white line* and *continuous white line* of the *right* image). The rate of atrophy enlargement (mm^2/y) was obtained as the atrophy enlargement (mm^2) divided by the follow-up time (years).

Mutation Screening

Mutation screening was performed using the single-stranded conformation polymorphism (SSCP) strategy in 35 subjects,[50] and the arrayed primer extension (APEX) microarray (ABCR400 chip; Asper Ophthalmics, Tartu, Estonia) in 33 patients.[51] All the variants detected were confirmed with direct Sanger sequencing. Direct Sanger sequencing also was performed in siblings of probands and parents when available to confirm segregation of alleles.

Nonnull variants were analyzed using two software prediction programs: Sorting Intolerant from Tolerance (SIFT, available in the public domain at http://sift.jcvi.org/),[52] and PolyPhen2 (available in the public domain at http://genetics.bwh.harvard.edu/pph/index.html).[53] All variants were compared to variants in the Exome Variant Server; National Heart, Lung, and Blood Institute (NHLBI) Exome Sequencing Project, Seattle, Washington (available in the public domain at http://snp.gs.washington.edu/EVS/).

Patients harboring two or more mutations were classified into two mutually exclusive genotype groups on the basis of the molecular analysis: patients with at least one null variant, (group A) and subjects with two or more missense variants (group B). Only patients harboring two or more likely disease-causing variants were included to investigate genotype-phenotype correlations. Null variants were those that would be expected to affect splicing, or to introduce a premature truncating codon in the protein if translated. One disease-associated intronic change with uncertain effect was treated as a null allele due to the associated severe clinical phenotype previously reported.[9,33]

Statistical Analysis

Statistical methods are provided in Supplementary Material S1.

RESULTS

Clinical Findings

We included in the study 68 patients with a clinical diagnosis of Stargardt disease. The clinical findings are summarized in Supplementary Table S1. There were 36 female (53%) and 32 male patients (47%). All complained of central visual loss, with a median age of onset of 19.0 years (range, 5–48 years) and a median duration of disease of 9.0 years (range, 0–47 years). One patient had relative foveal sparing in the left eye on AF imaging at presentation (patient 24; age of onset, 48 years). The median ages at baseline and at follow-up were 30.5 and 39.0 years (range, 8–58 and 18–67), respectively. The mean follow-up interval was 9.1 years (range, 6–13). Seven patients (10%) presented before 16 years of age and 61 patients (90%) presented after 16 years. The median logMAR visual acuities at baseline and at follow-up were 1.00 (range, 0.0–1.98) and 1.00 (0.0–2.28), respectively, with a median logMAR visual acuity reduction during the follow-up interval of 0.15 (range, –0.78–1.28).

Color fundus photographs and AF images of representative cases are shown in Figures 1 and 3; with three representative cases without AF type transition during follow-up in Figure 1, and two cases with AF type transition in Figure 3.

Fundus AF Findings

The AF imaging at baseline was obtained with the Zeiss system in 52 patients and with the HRA2 in 16 subjects. The AF imaging at follow-up was obtained with the HRA2 or Spectralis (field of view 30° × 30°) in all 68 individuals, with additional wide-field images (55° × 55°) undertaken in 19 patients. Complete AF data sets were available at baseline and follow-up with few exceptions; in patient 28, AF images were unavailable of the right eye at baseline and follow-up, and six patients

Investigative Ophthalmology & Visual Science